Electronic supplementary information

Molecular hydrogen and water activation by transition metal frustrated Lewis pairs containing ruthenium or osmium components: catalytic hydrogenation assays

Sophie Beard, Alejandro Grasa, Fernando Viguri, Ricardo Rodríguez, José A. López, Fernando J. Lahoz, Pilar García-Orduña, Pilar Lamata,* and Daniel Carmona*

Instituto de Síntesis Química y Catálisis Homogénea (ISQCH), CSIC - Universidad de Zaragoza, Departamento de Química Inorgánica, Pedro Cerbuna 12, 50009 Zaragoza, Spain. E-mail: dcarmona@unizar.es, plamata@unizar.es

Table of Contents

1 Preparation and characterization of the phosphano-thiourea ligand H$_2$L1

At RT, a mixture of 2-(diphenylphosphano)ethylamine (1.20 g, 5.23 mmol) and *p*-Tolyl-isothiocyanate (780.9 mg, 5.23 mmol) in dry THF (10 mL) was stirred for 15 h. The resulting solution was vacuum-evaporated to dryness. The residue was washed with *n*-hexane (3 × 5 mL). Evaporation of the solvent under vacuum gave the phosphano-thiourea compound as a white solid.
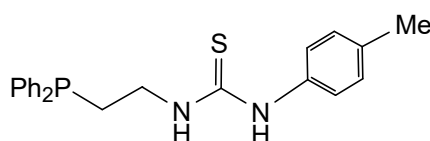

H$_2$L1

Yield: 1.93 g, 98 %. Anal. Calcd for C$_{22}$H$_{23}$N$_2$PS: C, 69.8; H, 6.1; N, 7.4; S, 8.5 Found: C, 69.55; H, 6.6; N, 7.4; S, 8.4. HRMS (*μ*-TOF), C$_{22}$H$_{24}$N$_2$PS, [M + H]$^+$, calcd: 379.1392, found: 379.1381. IR (cm^{-1}): ν(NH) 3319 (br), 3160 (br). ^{1}H NMR (500.10 MHz, CD$_2$Cl$_2$, RT): δ = 7.70 (s, 1H, *p*-TolylN*H*), 7.46-7.32 (m, 10H, PPh$_2$), 7.22, 7.05 (AB system, *J*(A,B) = 8.0 Hz, 4H, *p*-Tolyl), 6.24 (bs, 1H, N*H*CH$_2$), 3.74 (m, 2H, NCH$_2$), 2.41 (m, 2H, PCH$_2$), 2.36 (s, 3H, Me). ^{13}C{^{1}H} NMR (125.77 MHz, CD$_2$Cl$_2$, RT): δ = 181.57 (C=S), 138.65 (d, *J* = 12.6 Hz), 133.54, 133.39, 129.60, 129.36, 129.30 (PPh$_2$), 138.16 (CN), 134.27 (*C*Me), 131.63 (CH$_3$, CH$_5$), 126.44 (CH$_2$, CH$_6$) (*p*-Tolyl), 43.34 (d, *J* = 21.23 Hz, CH$_2$N), 28.93 (CH$_2$P), 21.86 (Me). ^{31}P{^{1}H} NMR (202.46 MHz, CD$_2$Cl$_2$, RT): δ = −21.20 (s).

2 Preparation and characterization of the complexes 1-4

*Preparation of the complexes [(Cym)MCl(κ^2S,P-**H₂L1**)][SbF₆] (M= Ru (**1**), Os(**2**))*

To a suspension of the dimer [{(Cym)MCl}₂(μ-Cl)₂] (0.25 mmol), in methanol (10 mL), 190.0 mg (0.50 mmol) of **H₂L1** and 129.9 mg (0.50 mmol) of NaSbF₆ were added. The resulting solution was stirred for 15 h and vacuum-evaporated to dryness. The residue was extracted with dichloromethane and the solution was concentrated under reduced pressure to *ca.* 2 mL. The slow addition of *n*-pentane led to the precipitation of an orange (ruthenium) or yellow (osmium) solid which was washed with *n*-pentane (3 × 5 mL) and vacuum-dried. Crystals of **2** suitable for X-ray diffraction analysis were obtained by crystallisation from CH₂Cl₂/*n*-hexane solutions.

1
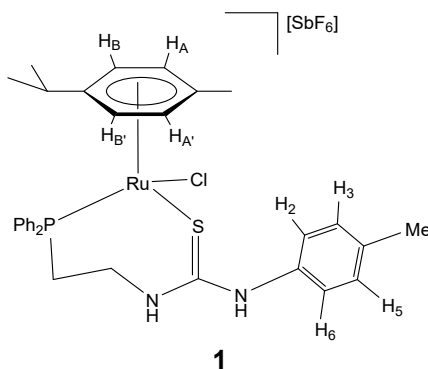
Complex 1. Yield: 407.0 mg, 92 %. Anal. Calcd for C₃₂H₃₇N₂ClF₆PRuSSb: C, 43.4; H, 4.2; N, 3.2; S, 3.6. Found: C, 43.6; H, 4.1; N, 3.2; S, 3.75. HRMS (μ-TOF), C₃₂H₃₇N₂ClPRu, [M – SbF₆]⁺, calcd: 649.1142, found: 649.1126. IR (cm⁻¹): ν(NH) 3335 (br), ν(SbF₆) 655 (s). ¹H NMR (500.10 MHz, CD₂Cl₂, RT): δ = 8.35 (s, 1H, *p*-TolylN*H*), 7.89-7.48 (m, 10H, PPh₂), 7.26 (bd, *J* = 7.4, 2H, H₃, H₅, *p*-Tolyl), 6.95 (bs, 2H, H₂, H₆, *p*-Tolyl), 6.56 (bs, 1H, CH₂N*H*), 5.74 (bs, 1H, H_B), 5.59 (bs, 1H, H_A), 5.20 (s, 2H, H_A', H_B'), 3.83 (bs, 1H, NCH₂), 3.43 (m, 1H, NCH₂), 3.02, 2.16 (2 × m, 2H, PCH₂), 2.51 (m, 1H, CH *i*Pr), 2.38 (s, 3H, Me *p*-Tolyl), 1.88 (s, 3H, Me Cym), 1.23 (bs, 3H, Me *i*Pr), 0.95 (bs, 3 H, Me *i*Pr). ¹³C{¹H} NMR (125.77 MHz, CD₂Cl₂, RT): δ = 135.76-129.73 (PPh₂), 131.75 (CH₃, CH₅, *p*-Tolyl), 126.55 (CH₂, CH₆, *p*-Tolyl), 93.92

(CH$_A$), 91.30 (CH$_B$), 90.02, 89.19 (CH$_{A'}$, CH$_{B'}$), 30.78 (CH iPr), 22.59, 22.07 (Me iPr), 21.66 (Me p-Tolyl), 17.85 (Me Cym). ^{31}P{^{1}H} NMR (202.46 MHz, CD$_2$Cl$_2$, RT): δ = 23.65 (vbs).

^{31}P{^{1}H} NMR (202.46 MHz, CD$_2$Cl$_2$, 173 K): δ = 35.91 (s) major, 19.39 (s) minor.
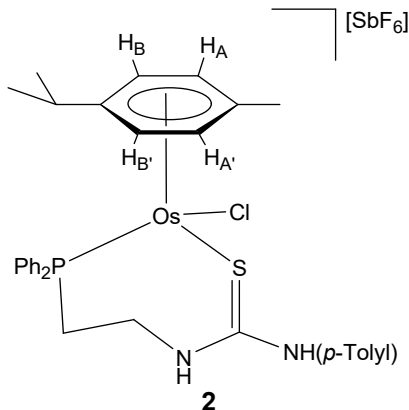
Complex 2. Yield: 457.8 mg, 94 %. Anal. Calcd for C$_{32}$H$_{37}$N$_2$ClF$_6$OsPSSb: C, 39.5; H, 3.8; N, 2.9; S, 3.3. Found: C, 39.3; H, 3.9; N, 2.7; S, 3.3. HRMS (μ-TOF), C$_{32}$H$_{37}$N$_2$ClOsPS, [M $-$ SbF$_6$]$^+$, calcd: 739.1702, found: 739.1700. IR (cm^{-1}): ν(NH) 3238-3417 (br), ν(SbF$_6$) 659 (s).

Major isomer. ^{1}H NMR (500.10 MHz, CD$_2$Cl$_2$, 193 K): δ = 8.45 (s, 1H, p-TolylNH), 7.85-7.07 (m, 10H, PPh$_2$), 7.06 (d, J = 7.5 Hz, 2H), 6.48 (d, J = 8.3 Hz, 2H, p-Tolyl), 6.07 (bs, 1H, CH$_2$NH), 5.77 (d, J = 5.6 Hz, 1H, H$_B$), 5.69 (d, 1H, H$_A$), 5.07 (d, J = 7.6 Hz, 2H, H$_{A'}$, H$_{B'}$), 4.42, 3.42 (2 × m, 2H, NCH$_2$), 2.90, 2.59 (2 × m, 2H, PCH$_2$), 2.31 (m, 1H, CH iPr), 2.21, (s, 3H, Me p-Tolyl), 1.88 (s, 3H, Me Cym), 1.12 (d, J = 6.4 Hz, 3H, Me iPr), 0.85 (d, J = 6.1 Hz, 3H, Me iPr). ^{13}C{^{1}H} NMR (125.77 MHz, CD$_2$Cl$_2$, 193K): δ = 177.63 (C=S), 135.87 (d, J = 55.0), 127.87 (d, J = 53.5), 132.29-126.71 (PPh$_2$), 138.89, 130.72 (CH$_3$, CH$_5$, p-Tolyl), 130.83, 124.51 (CH$_2$, CH$_6$, p-Tolyl), 108.73 (C−Me, Cym), 94.55 (C−iPr, Cym), 85.17 (CH$_B$), 81.79 (CH$_A$), 81.34 (CH$_{B'}$), 79.73 (CH$_{A'}$), 42.80 (CH$_2$N), 29.14 (CH iPr), 27.72 (d, J = 35.8, CH$_2$P), 21.76, 21.49 (Me iPr), 21.05 (Me p-Tolyl), 17.00 (Me Cym). ^{31}P{^{1}H} NMR (202.46 MHz, CD$_2$Cl$_2$, 193K): δ = −8.22 (s).

Minor isomer. ^{1}H NMR (500.10 MHz, CD$_2$Cl$_2$, 193 K): δ = 8.35 (s, 1H, p-TolylNH), 7.85-7.07 (m, 10H, PPh$_2$), 5.69, 5.62, 5.37, 5.20 (4 × bd, 4H, H$_A$, H$_B$, H$_{A'}$, H$_{B'}$), 3.42, 3.14, 3.05, 2.59

(4 × m, 4H, CH$_2$CH$_2$), 1.88 (m, 1H, CH iPr), 1.03 (bd, J = 5.3 Hz, 3H, Me iPr), 0.66 (bd = 5.07

Hz, 3H, Me iPr). ^{13}C{^{1}H} NMR (125.77 MHz, CD$_2$Cl$_2$, 193K): δ = 177.41(C=S), 140.08,

130.47 (p-Tolyl), 103.42, 93.31 (C−Me, C−iPr, Cym), 84.79, 82.88, 78.92, 77.89 (CH$_A$, CH$_B$,

CH$_{A'}$, CH$_{B'}$), 39.76 (CH$_2$N), 28.54 (CH iPr), 21.85, 21.24 (Me iPr). ^{31}P{^{1}H} NMR (202.46

MHz, CD$_2$Cl$_2$, 193K): δ = −23.84 (s).

^{31}P{^{1}H} NMR (202.46 MHz, CD$_2$Cl$_2$, RT): δ = −16.50 (s).

*Preparation of the complexes [(Cym)M(κ^3S,P,N-**H$_2$L1**)][SbF$_6$]$_2$ (M= Ru (**3**), Os(**4**))*

To a solution of the corresponding chlorido complex [(Cym)MCl(κ^2S,P-**H$_2$L1**)][SbF$_6$] (0.17

mmol) in acetone (10 mL), 65.9 mg (0.19 mmol) of AgSbF$_6$ were added. The resulting

suspension was stirred for 2 h and kept for 3 days at −20 ºC. The AgCl formed was separated

with cannula and the filtrate was concentrated under reduced pressure to *ca*. 2 mL. The slow

addition of *n*-pentane led to the precipitation of an orange (complex **3**) or yellow (complex **4**)

solid, which was washed with *n*-pentane (3 × 5 mL) and vacuum-dried. Crystals of **4** suitable

for X-ray diffraction analysis were obtained by crystallisation from CH$_2$Cl$_2$/*n*-hexane solutions.

3
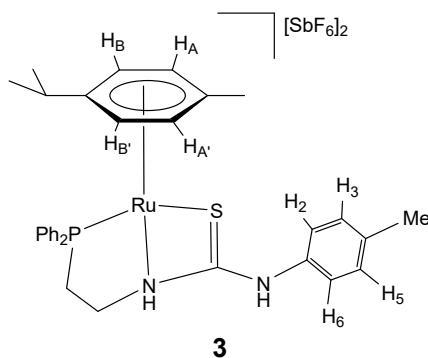
Complex 3. Yield: 145.7 mg, (79 %). Anal. Calcd for C$_{32}$H$_{37}$N$_2$F$_{12}$PRuSSb$_2$: C, 35.4; H, 3.4;

N, 2.6; S, 2.95. Found: C, 35.8; H, 3.7; N, 2.5; S, 2.8. HRMS (μ-TOF), C$_{32}$H$_{36}$N$_2$PRuS, [M − 2

SbF$_6$ − H]$^+$, calcd: 613.1375, found: 613.1376. IR (cm^{-1}): ν(NH) 3120-3415 (vbr), ν(SbF$_6$) 652

(s). ^{1}H NMR (500.10 MHz, CD$_2$Cl$_2$, RT) δ = 8.20 (vbs, NH), 7.70-7.37 (m, 10H, PPh$_2$), 7.34

(A part of an AB system, 2H, H$_2$, H$_6$, *p*-Tolyl), 7.27 (B part of an AB system, J(A,B) = 7.9 Hz,

2H, H$_3$, H$_5$, *p*-Tolyl), 6.00, 5.97 (2 × bs, 2H, H$_A$, H$_B$), 5.78 (bd, 1H, H$_{B'}$), 5.49 (bd, *J* = 5.8 Hz, 1H, H$_{A'}$), 4.18 (dm, *J* = 38.6 Hz, 1H, NCH$_2$), 3.36 (m, 1H, NCH$_2$), 3.08, 2.61 (2 × m, 2H, PCH$_2$), 2.36 (s, 3H, Me *p*-Tolyl), 2.33 (m, 1H, CH *i*Pr), 1.80 (s, 3H, Me Cym), 1.21 (d, *J* = 7.1 Hz, 3H, Me *i*Pr), 1.15 (d, *J* = 7.0 Hz, 3H, Me *i*Pr). ^{13}C{^{1}H} NMR (125.77 MHz, CD$_2$Cl$_2$, RT): *δ* = 187.29 (C=S), 134.48-129.70 (PPh$_2$), 140.94 (*C*Me), 134.01 (CN), 131.39 (CH$_3$, CH$_5$), 123.42 (CH$_2$, CH$_6$) (*p*-Tolyl), 116.39 (*C*−Me, Cym), 105.19 (*C*−*i*Pr, Cym), 92.32 (CH$_{A'}$), 89.02 (CH$_{B'}$, CH$_A$, CH$_B$), 57.70 (CH$_2$N), 32.03 (CH *i*Pr), 25.27 (CH$_2$P), 23.22, 22.95 (Me *i*Pr), 21.83 (Me *p*-Tolyl), 18.47 (Me Cym). ^{31}P{^{1}H} NMR (202.46 MHz, CD$_2$Cl$_2$, RT): *δ* = 60.81 (bs).

4
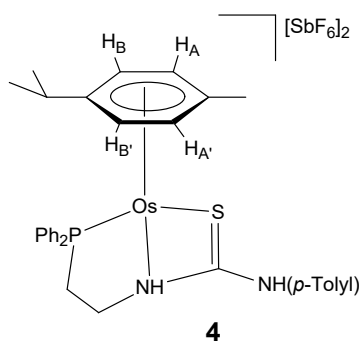
Complex 4. Yield: 173.7 mg, (87 %). Anal. Calcd for C$_{32}$H$_{37}$N$_2$F$_{12}$OsPSSb$_2$: C, 32.7; H, 3.2; N, 2.4; S, 2.7. Found: C, 32.5; H, 3.2; N, 2.3; S, 2.6. HRMS (*µ*-TOF), C$_{32}$H$_{36}$N$_2$OsPS, [M − H − 2 SbF$_6$]$^+$, calcd: 703.1945, found: 703.1938. IR (cm^{-1}): ν(NH) 3080-3430 (vbr), ν(SbF$_6$) 652 (s). ^{1}H NMR (500.10 MHz, CD$_2$Cl$_2$, RT): *δ* = 8.40 (bs, NH), 7.72-7.31(m, 10H, PPh$_2$), 7.43-7.29 (m, 4H, *p*-Tolyl), 6.14 (d, *J* = 5.9 Hz, 1H, H$_A$), 6.10 (d, *J* = 5.8 Hz, 1H, H$_{B'}$), 6.04 (d, 1H, H$_B$), 5.67 (d, 1H, H$_{A'}$), 4.23 (dm, *J* = 36.6 Hz, 1H, NCH$_2$), 3.36 (m, 1H, NCH$_2$), 2.99, 2.67 (2 × m, 2H, PCH$_2$), 2.36 (s, 3H, Me *p*-Tolyl), 2.17 (m, 1H, CH *i*Pr), 1.89 (s, 3H, Me Cym), 1.21 (d, *J* = 7.0 Hz, 3H, Me *i*Pr), 1.15 (d, *J* = 7.0 Hz, 3H, Me *i*Pr). ^{13}C{^{1}H} NMR (125.77 MHz, CD$_2$Cl$_2$, RT): *δ* = 191.09 (C=S), 142.00, 131.42 (CH$_3$, CH$_5$), 130.35, 123.15 (CH$_2$, CH$_6$) (*p*-Tolyl), 134.79-130.60, 133.40 (d, *J* = 58.3), 128.60 (d, *J* = 64.3) (PPh$_2$), 110.29 (*C*−Me, Cym), 99.59 (*C*−*i*Pr, Cym), 84.45, 84,41 (CH$_B$, CH$_{A'}$), 80.39 (CH$_A$), 76.32 (CH$_{B'}$), 61.48 (CH$_2$N),

31.48 (CH iPr), 25.61 (d, J = 35.7, CH$_2$P), 23.23, 23.16 (Me iPr), 21.86 (Me p-Tolyl), 18.32 (Me Cym). ^{31}P{^{1}H} NMR (202.46 MHz, CD$_2$Cl$_2$, RT): δ = 26.96 (s).

3 Kinetic studies for the H/D exchange at the Cym methyl protons of complex 7

Kinetic experiments were carried out in an NMR tube. Determination of observable kinetic constants were accomplished by ^{1}H NMR integration of the Me(Cym) hydrogens *versus* time, using the methyl groups, Me(*p*-Tolyl), as internal reference. Kinetic parameters ($\Delta H^{\ddagger}$, $\Delta S^{\ddagger}$, $\Delta G^{\ddagger}$) were obtained through Eyring analysis; $\ln(k_{obs}/T) = -\Delta H^{\ddagger}/RT + \ln(k_B/h) + (\Delta S^{\ddagger}/R)$.

Kinetic experiment at 373 K: [CymRu(κ^3P,N,N'-HL2)][SbF$_6$] (17.99 mM) in 0.35/0.10 mL of THF-d_8/D$_2$O

y = -2,3216E-04x + 4,0440E+00
R² = 9,9584E-01
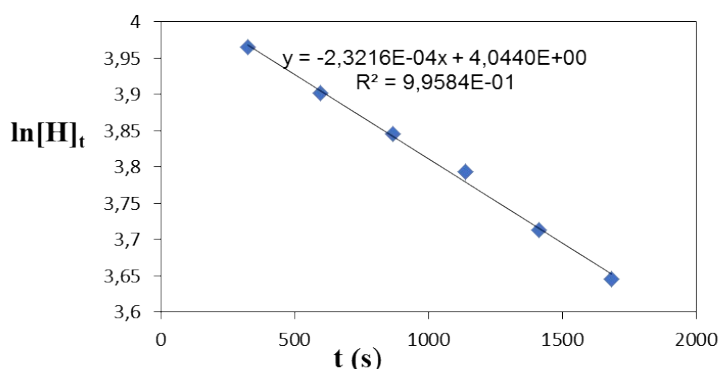
t (s)	ln[H]
0	3.988373643
326	3.964763777
597	3.901362266
867	3.845272799
1138	3.793979505
1414	3.713936797
1684	3.645883334

Kinetic experiment at 368 K: [CymRu(κ^3P,N,N'-HL2)][SbF$_6$] (18.11 mM) in 0.35/0.10 mL of THF-d_8/D$_2$O

y = -1,2966E-04x + 4,0216E+00
R² = 9,9635E-01
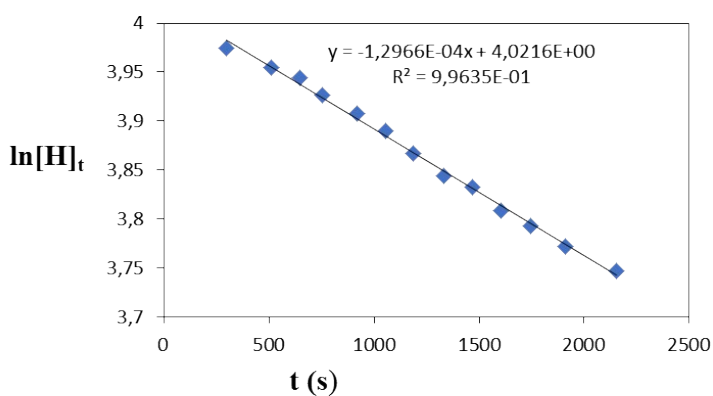
t (s)	ln[H]
0.00	3.9950536
299.00	3.9748509
510.00	3.9542317
646.00	3.9437604
755.00	3.9260608
918.00	3.9080423
1056.00	3.8896931
1189.00	3.8672203
1333.00	3.8442308
1469.00	3.8325347
1606.00	3.8087241
1743.00	3.7925294
1908.00	3.7719101
2153.00	3.7465923
2423.00	3.6525633

Kinetic experiment at 363 K: [CymRu(κ³*P*,*N*,*N*'-HL2)][SbF₆] (18.16 mM) in 0.35/0.10 mL of THF-*d*₈/D₂O

$$y = -7,3601E-05x + 3,9972E+00$$
$$R^2 = 9,9747E-01$$
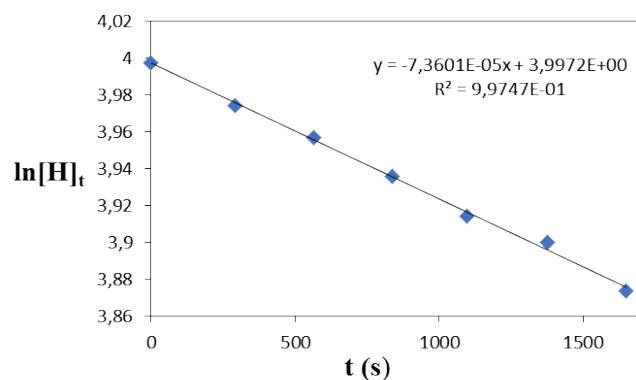
t (s)	ln[H]
0	3.997713271
293	3.974103405
564	3.956891276
839	3.935837867
1096	3.914331662
1378	3.899732862
1651	3.873660622

Kinetic experiment at 358 K: [CymRu(κ³*P*,*N*,*N*'-HL2)][SbF₆] (18.33 mM) in 0.35/0.10 mL of THF-*d*₈/D₂O

$$y = -3,8773E-05x + 4,0144E+00$$
$$R^2 = 9,9421E-01$$
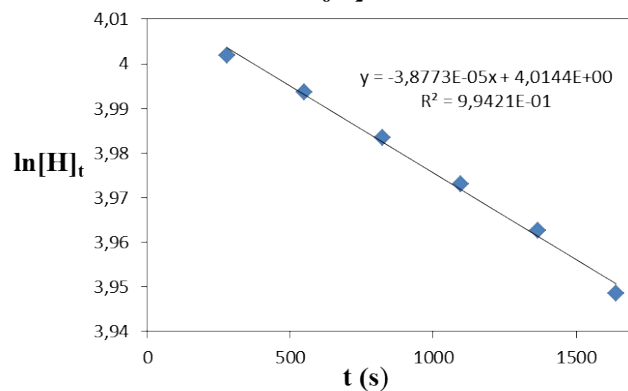
t (s)	ln[H]
0.00	4.0069665
279	4.0019539
551	3.9935435
824	3.9833566
1097	3.9730649
1367	3.9626662
1641	3.9486309

Eyring analysis

y = -1.54885E+04x + 2.72367E+01
R² = 9.99655E-01

$\ln(k_{obs}/T)$

1/T
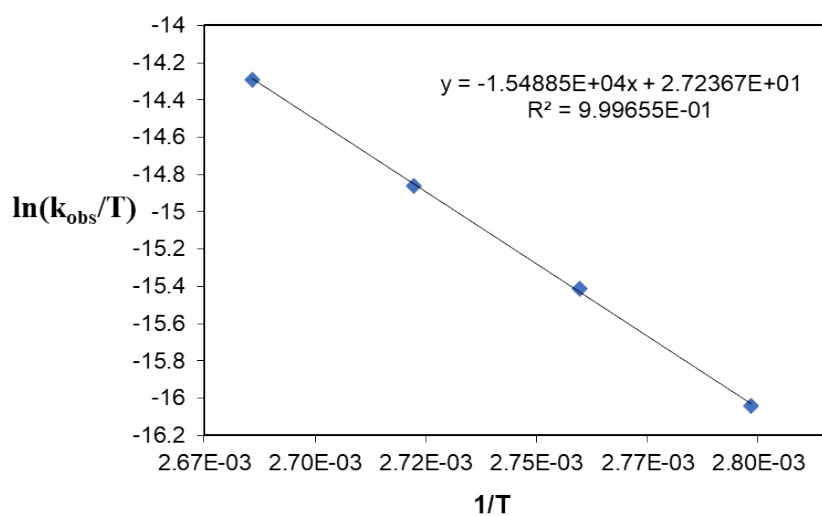
T	k (mM/s)	(1/T)	ln(k/T)
373	2.32E-04	0.002680965	-1.43E+01
368	1.30E-04	0.002717391	-1.49E+01
363	7.36E-05	0.002754821	-1.54E+01
358	3.88E-05	0.002793296	-1.60E+01

$\Delta H^{\neq}$	$\Delta S^{\neq}$	$\Delta G^{\neq}$ (273K)
30.78 ± 0.40 Kcal/mol	6.91 ± 1.1 cal/mol	28.75 ± 0.73 Kcal/mol

4 NMR and DFT studies on the fluxionality of the complexes 5, 6, 11 and 12

The variable temperature $^{31}P\{^1H\}$ NMR spectra of complexes **5**, **6**, **11** and **12** (Fig. S1) indicate that they are fluxional.
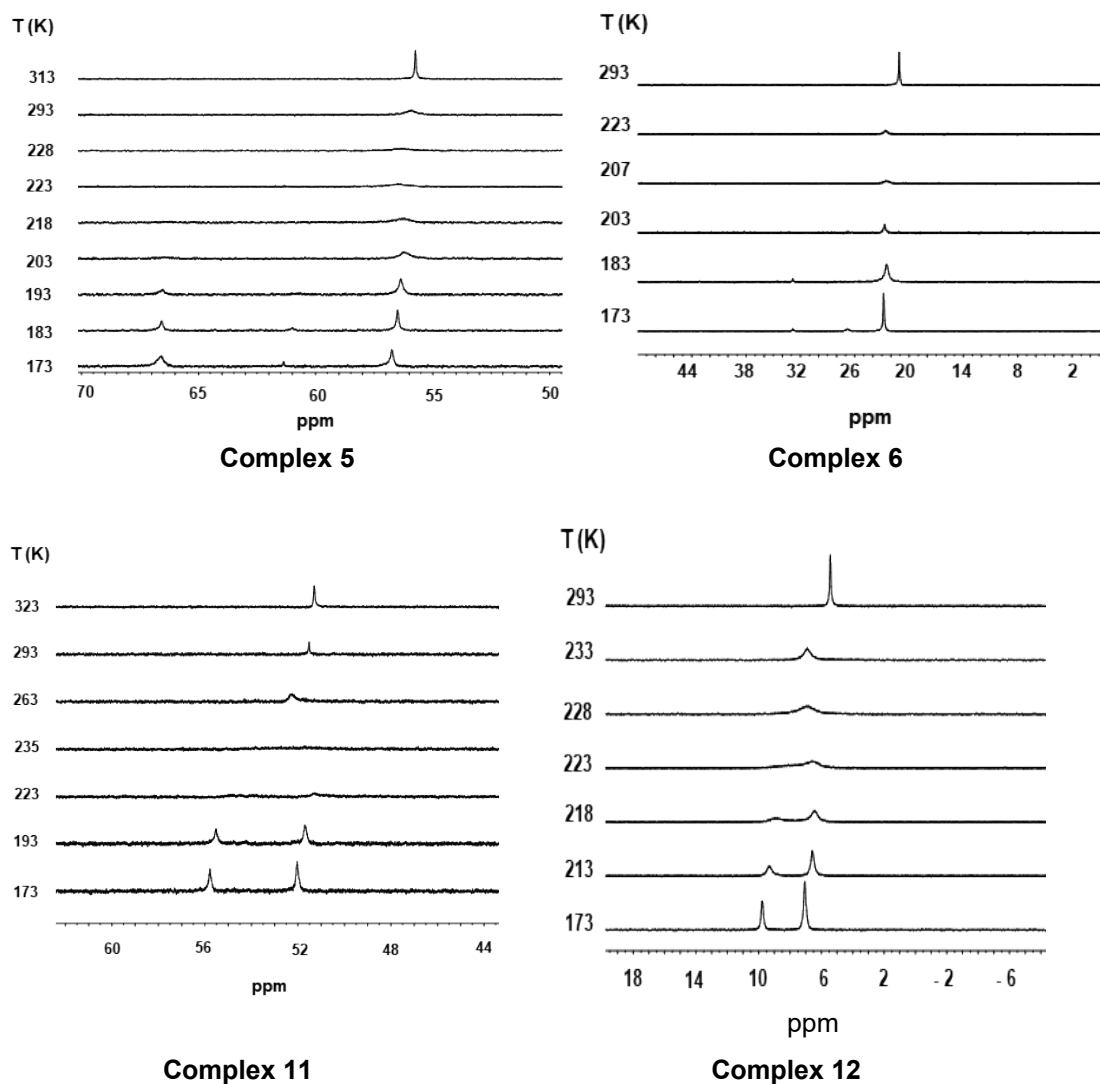
Fig. S1 Variable temperature $^{31}P\{^1H\}$ NMR spectra (202.46 MHz, CD_2Cl_2)

For complex **5**, analysis of the temperature evolution of the singlet recorded at 313 K gives an activation energy at the coalescence temperature of 9.50 ± 0.12 kcal·mol^{-1}. Additionally, below 193 K a new signal at about 61.4 ppm appeared. To account for these experimental data, the four rotamers depicted in Fig. S2 were considered (data taken from the crystal structure of complex **5**). From DFT calculations, the energy barrier for the interconversions **5a1 ↔ 5a2, 5b1 ↔ 5b2, 5a1 ↔ 5b1** and **5a2 ↔ 5b2** are 6.4, 7.2, 10.3 and 11.1 kcal mol^{-1}, respectively

(Fig. S3). The four isomers are unequally populated according to the relative Gibbs free energy values calculated that are quoted in Fig. S3. The calculated energy barrier for the rotation around the arene centroid-metal axis (6.4 and 7.2 kcal mol^{-1}) is close to the minimum value that allows achieve the required temperature to frozen the involved movement and, therefore, to detect by NMR spectroscopy the implicated individual species.[S1]
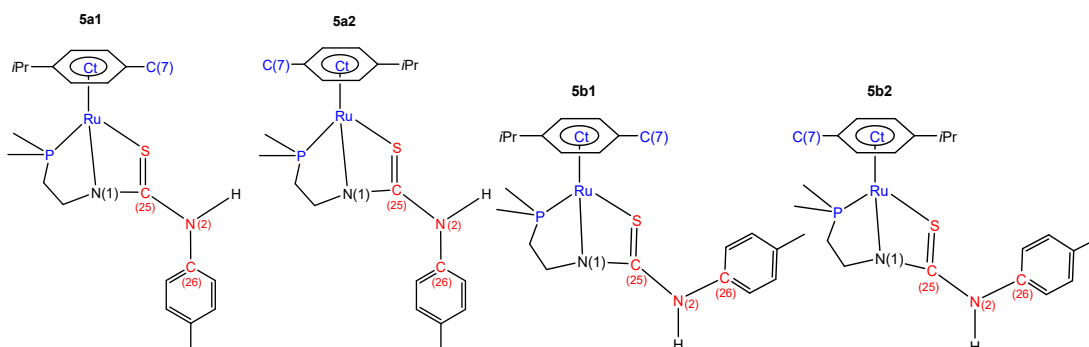
Fig. S2 Schematic representation of the rotamers **5a1,2** and **5b1,2**. Dihedral angles (º): **5a1**, C(7)−Ct−Ru−P: 101.7, S−C(25)−N(2)−C(26): 158.6; **5a2**, C(7)−Ct−Ru−P: −50.1, S−C(25)−N(2)−C(26): 158.7; **5b1**, C(7)−Ct−Ru−P: 103.9, S−C(25)−N(2)−C(26): −8.4; **5b2**, C(7)−Ct−Ru−P: −46.1, S−C(25)−N(2)−C(26): −8.0. Ct stands for the centroid of the Cym ligand. For the atom labelling, see Fig. 1 in Results and Discussion section).
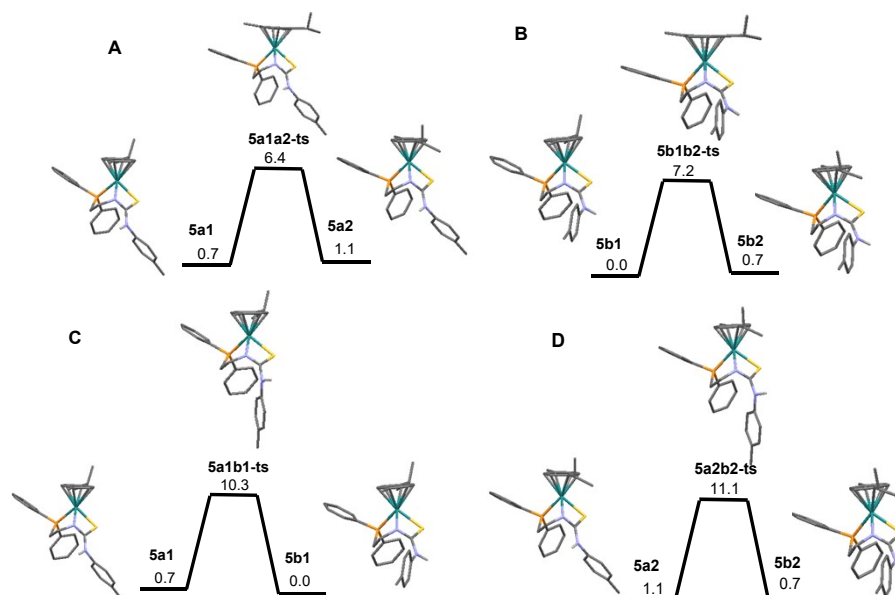
Fig. S3 Gibbs free energy profile of the equilibrium between isomers **5a1** and **5a2** (**A**), **5b1** and **5b2** (**B**), and rotamers **5a1** and **5b1** (**C**), **5a2** and **5b2** (**D**). For clarity, hydrogen atoms have been omitted, except the NH proton. Free energies are in kcal mol^{-1}.

(Fig. S3). The four isomers are unequally populated according to the relative Gibbs free energy values calculated that are quoted in Fig. S3. The calculated energy barrier for the rotation around the arene centroid-metal axis (6.4 and 7.2 kcal mol^{-1}) is close to the minimum value that

allows achieve the required temperature to frozen the involved movement and, therefore, to detect by NMR spectroscopy the implicated individual species.[S1]

A plausible explanation is as follows: at the lowest temperature recorded, 173 K, only one of the two rotations around the arene centroid-metal axis processes considered (**5a1** ↔ **5a2** or **5b1** ↔ **5b2**) is fast. However, at this temperature, the other three exchange processes proposed should be essentially frozen. One of the three $^{31}P\{^1H\}$ NMR singlets observed at 173 K can be assigned to the average of the two rotamers involved in the exchange active at this temperature. The two other $^{31}P\{^1H\}$ NMR singlets can be attributed to each one of the two remaining rotamers that are in the slow exchange regime on the NMR time scale. Heating up to 193 K, rotation around the arene centroid-metal axis of both species becomes free and consequently from 193 K onwards, the $^{31}P\{^1H\}$ NMR spectrum of the sample consists of only two singlets. At about 222 K these two singlets coalesce which gives an $\Delta G^{\#}$ value for the process at this temperature of 9.50 kcal mol^{-1}, in good agreement with the calculated values, 10.3 and 11.1 kcal mol^{-1}, for the rotation about the C(25)−N(2) bond. Above 222 K equilibration by rotation around this bond also becomes fast and, hence, the spectrum consists of a unique singlet.

Complex **6** shows comparable $^{31}P\{^1H\}$ NMR behaviour and similar activation energy at the coalescence temperature (8.89 ± 0.12 kcal·mol^{-1}) than complex **5**. Therefore, probably, it undergoes a similar dynamic process in solution.

Evolution with temperature of the $^{31}P\{^1H\}$ NMR spectrum of complexes **11** and **12** (Fig. S1) follows a common pattern, characteristic of a two-site exchange process: one unique singlet at high temperature broadens, coalesces and splits into two singlets. The activation energies at the coalescence temperature are 10.16 ± 0.12 and 10.02 ± 0.12 kcal·mol^{-1}, for complexes **11** and **12**, respectively.

To carry out DFT calculations, we have taken compound **2** as a model since its crystal structure has been determined by X-ray diffraction analysis (see Fig. S5, page S44) and, as in compounds **11** and **12**, in complex **2**, the phosphano-thiourea ligand coordinates to the metal forming a seven-membered metalacycle. As potentially responsible for the observed dynamic behaviour, a conformational change within the seven-membered metalacycle (**A** ↔ **B**) and an *s-cisoide* to *s-transoide* rotation around the C−N bond of the phosphano-thiourea ligand (**2a** ↔ **2b**) were examined (Fig. S4).
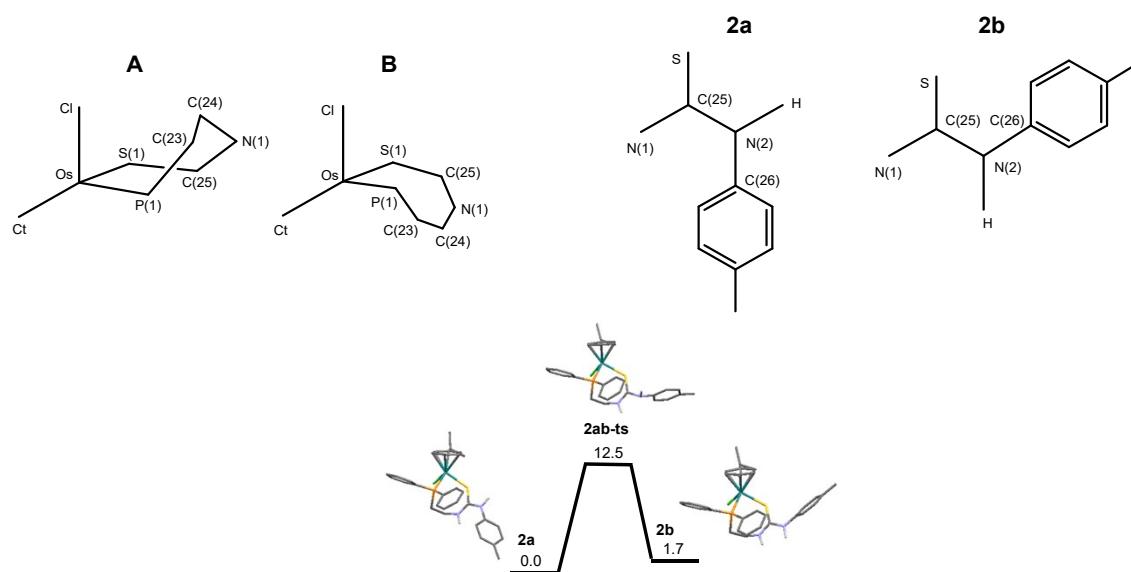
Fig. S4 A, **B**: Schematic representation of two conformations of the seven-membered metalacycle of complex **2** (see Fig. S5, page S44).
2a, **2b**: Schematic representation of a selected fragment of two rotamers around the C−N bond of the phosphano-guanidino ligand in complex **2**.
Gibbs free energy profile for the equilibrium between **2a** and **2b**. For clarity, hydrogen atoms have been omitted, except the NH protons. Free energies are in kcal mol^{-1}.

The performed DFT calculations give a barrier of 8.9 kcal·mol^{-1} for the interconversion from conformation **A** to conformation **B** and establish that conformer **B** is about 1.8 kcal·mol^{-1} less stable than conformer **A**. The calculated energy barrier fits well the experimental value obtained by NMR spectroscopy (see above), but the 1/4, **B**/**A** population ratio, measured by $^{31}P\{^{1}H\}$ NMR spectroscopy, is inconsistent with the calculated energy gap between the two conformers. On the other hand, an activation barrier of 12.5 kcal·mol^{-1} for the **2a** → **2b** interconversion and a Gibbs free energy difference between **2b** and **2a** of 1.7 kcal·mol^{-1} was

obtained. Again, the calculated energy barrier fits well the NMR experimental value obtained, but the population ratio measured by $^{31}P\{^1H\}$ NMR is not as expected for the calculated energy gap between the two rotamers. In summary, the theoretical calculations do not explain satisfactorily the fluxional process observed.

––––––––––

S1   J. K. Faller, *Comprehensive Organometallic Chemistry III*, Vol. 1. Eds.: R. H. Crabtree, D. M. P. Mingos, Elsevier, Oxford, 2007, p. 409.

5 NMR spectra of the ligand H$_2$L1 and of the complexes 1-6 and 11-19

* Denotes solvent

The spectra of the hydrido complexes **11-16** (Pages S25-S31) have been recorded under hydrogen pressure

^{1}H NMR of H$_2$L1 (500.10 MHz, CD$_2$Cl$_2$, RT)
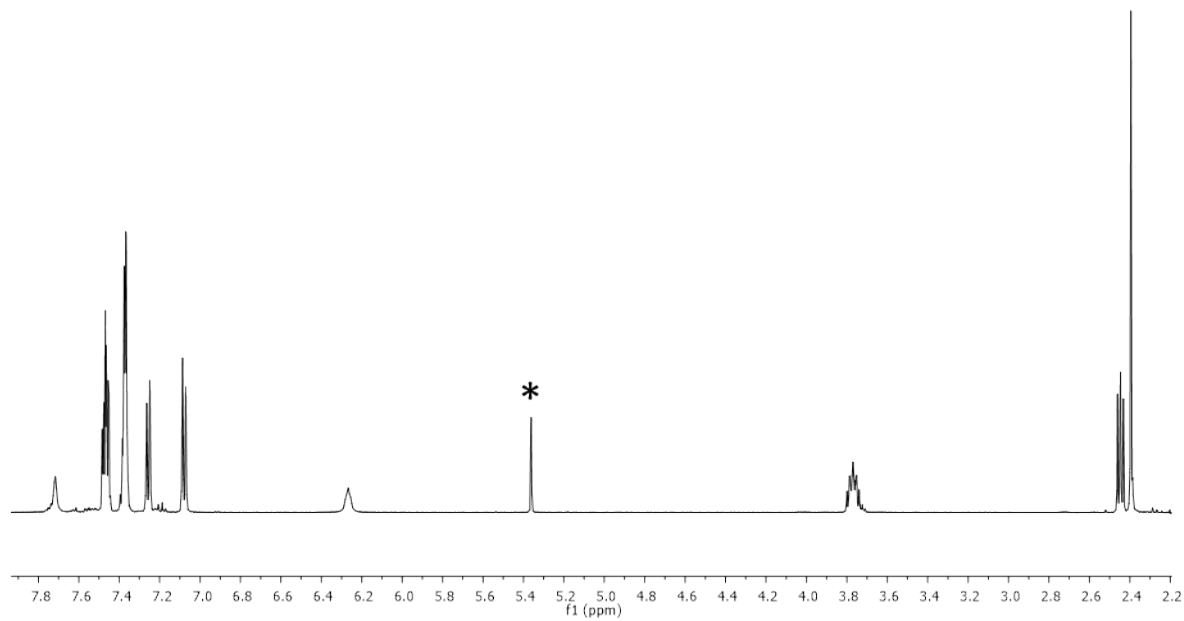
^{13}C{^{1}H} NMR of H$_2$L1 (125.77 MHz, CD$_2$Cl$_2$, RT)

³¹P{¹H} NMR of H₂L1 (202.46 MHz, CD₂Cl₂, RT)

$$^{31}\text{P}\{^{1}\text{H}\}\ \text{NMR of H}_2\text{L1 (202.46 MHz, CD}_2\text{Cl}_2\text{, RT)}$$
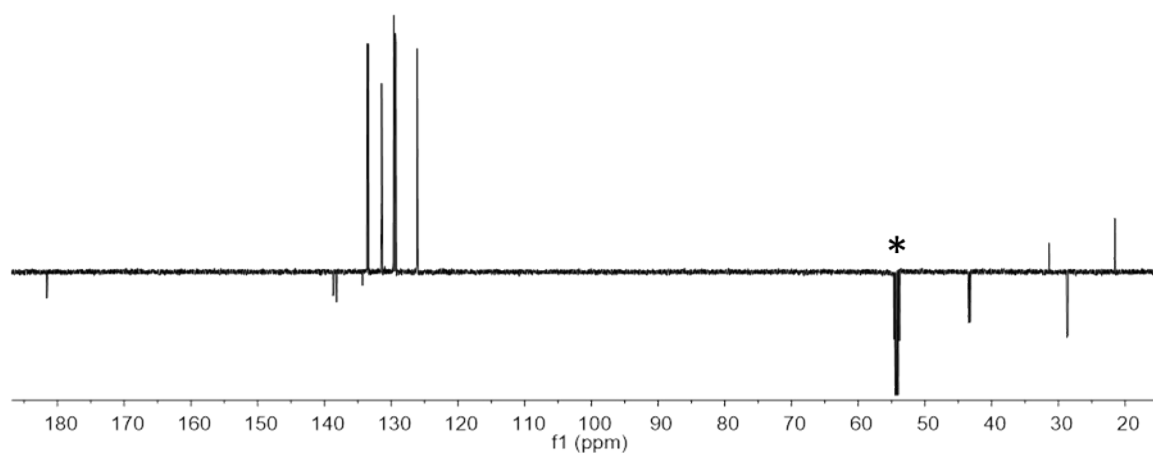
¹H NMR of [(Cym)RuCl(κ²*P*,*S*-H₂L1)][SbF₆] (1) (500.10 MHz, CD₂Cl₂, RT)
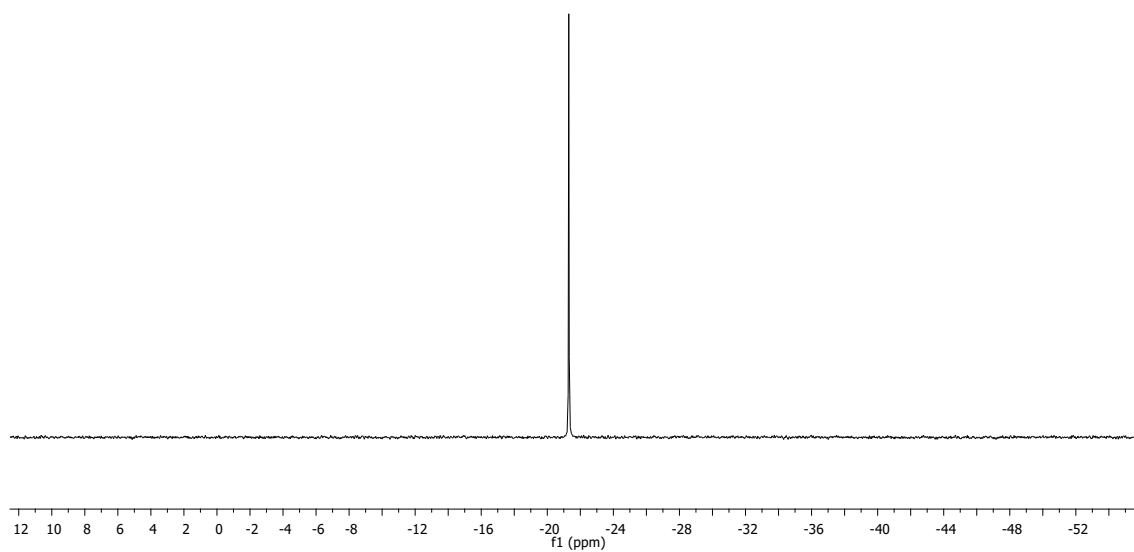
$$^{1}\text{H NMR of [(Cym)RuCl(}\kappa^{2}P,S\text{-H}_2\text{L1)][SbF}_6\text{] (1) (500.10 MHz, CD}_2\text{Cl}_2\text{, RT)}$$
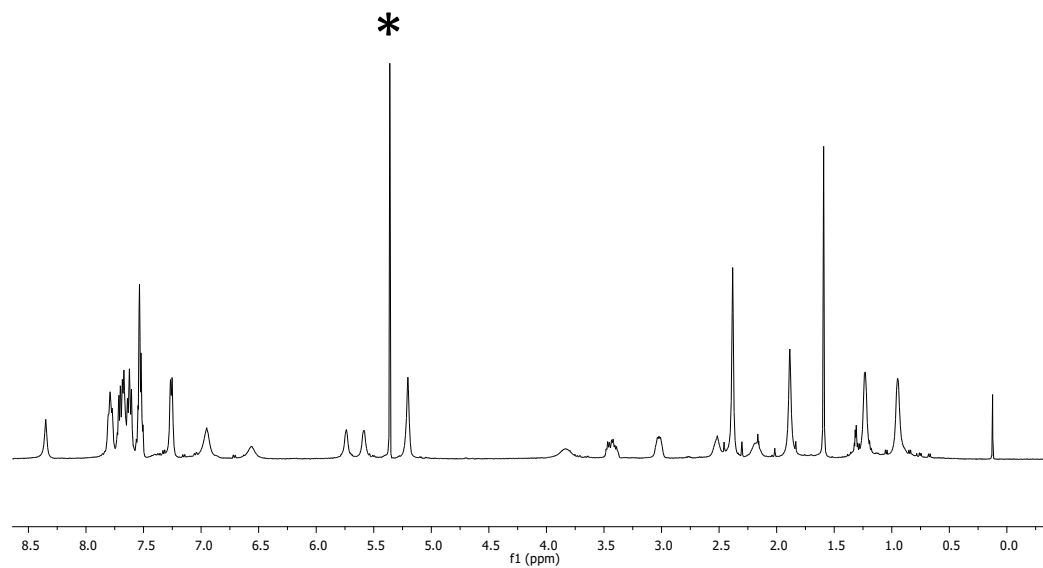
^{13}C{^{1}H} NMR of [(Cym)RuCl(κ^{2}P,S-H$_2$L1)][SbF$_6$] (1) (125.77 MHz, CD$_2$Cl$_2$, RT)

^{31}P{^{1}H} NMR of [(Cym)RuCl(κ^{2}P,S-H$_2$L1)][SbF$_6$] (1) (202.46 MHz, CD$_2$Cl$_2$, RT)

^{31}P{^{1}H} NMR of [(Cym)RuCl(κ^{2}P,S-H$_2$L1)][SbF$_6$] (1) (202.46 MHz, CD$_2$Cl$_2$, 173 K)
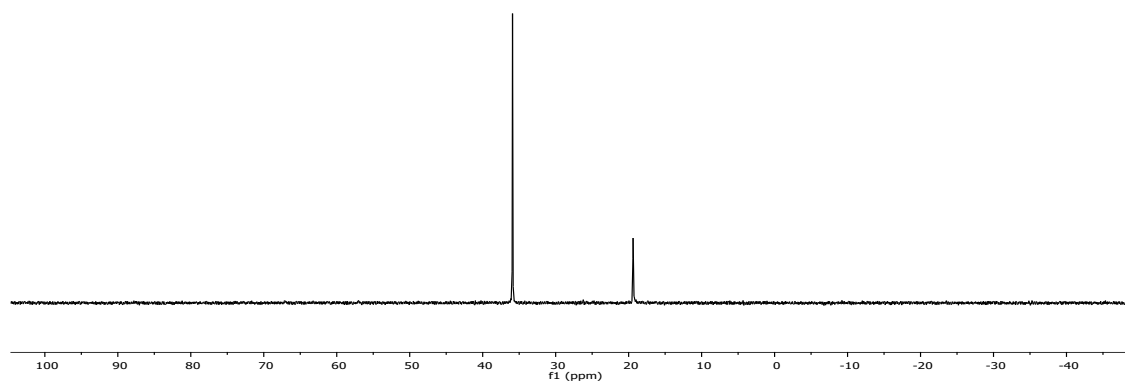
¹H NMR of [(Cym)OsCl(κ²P,S-H₂L1)][SbF₆] (2) (500.10 MHz, CD₂Cl₂, 193K)
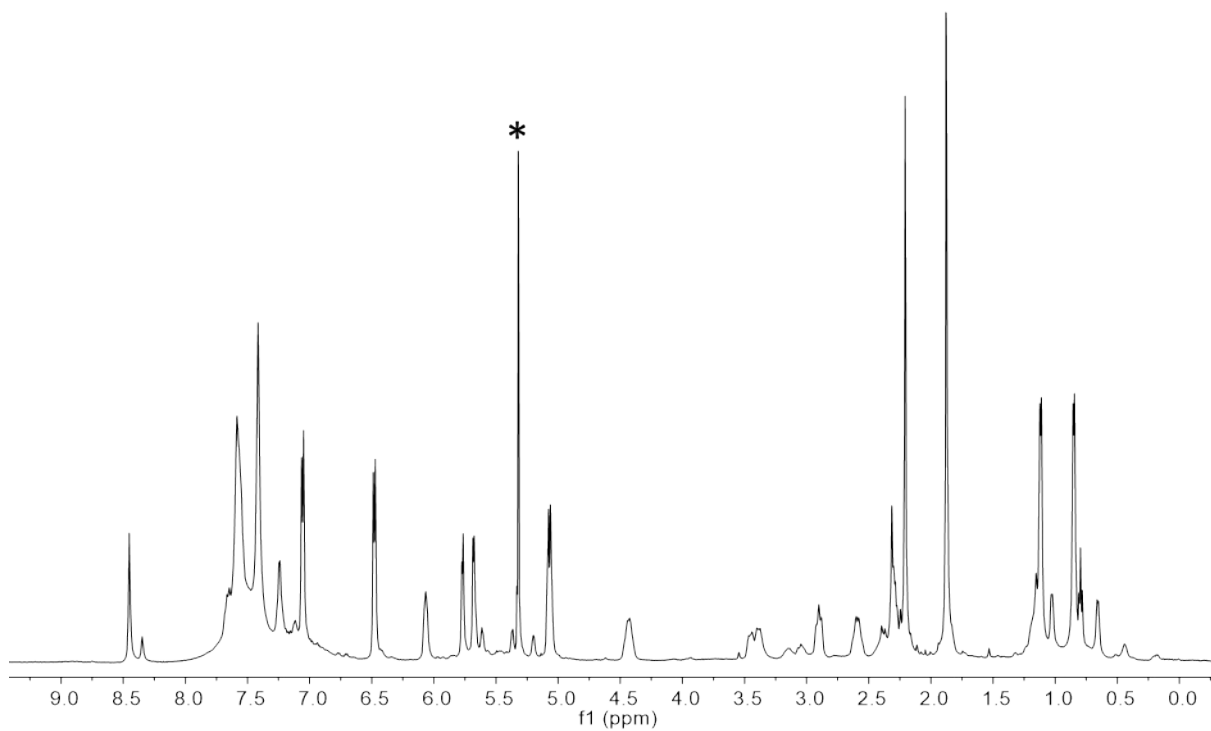
¹³C{¹H} NMR of [(Cym)OsCl(κ²P,S-H₂L1)][SbF₆] (2) (125.77 MHz, CD₂Cl₂, 193K)
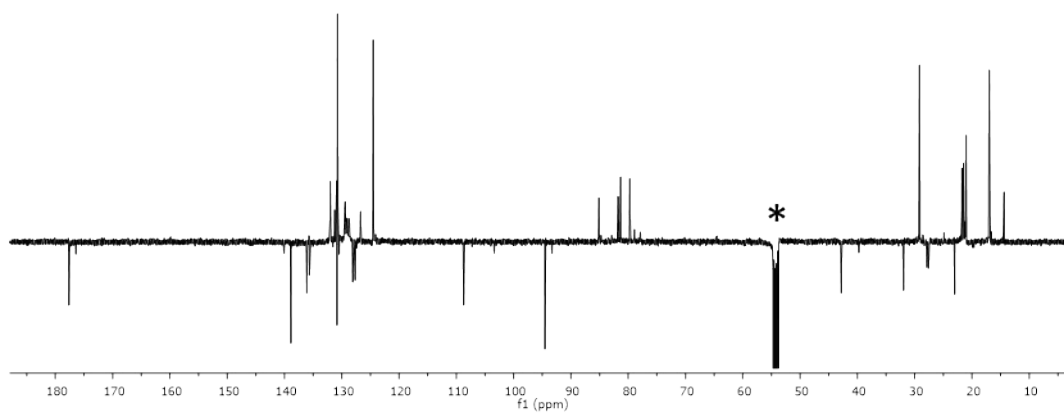
^{31}P{^{1}H} NMR of [(Cym)OsCl(κ^2P,S-H$_2$L1)][SbF$_6$] (2) (202.46 MHz, CD$_2$Cl$_2$, 193K)
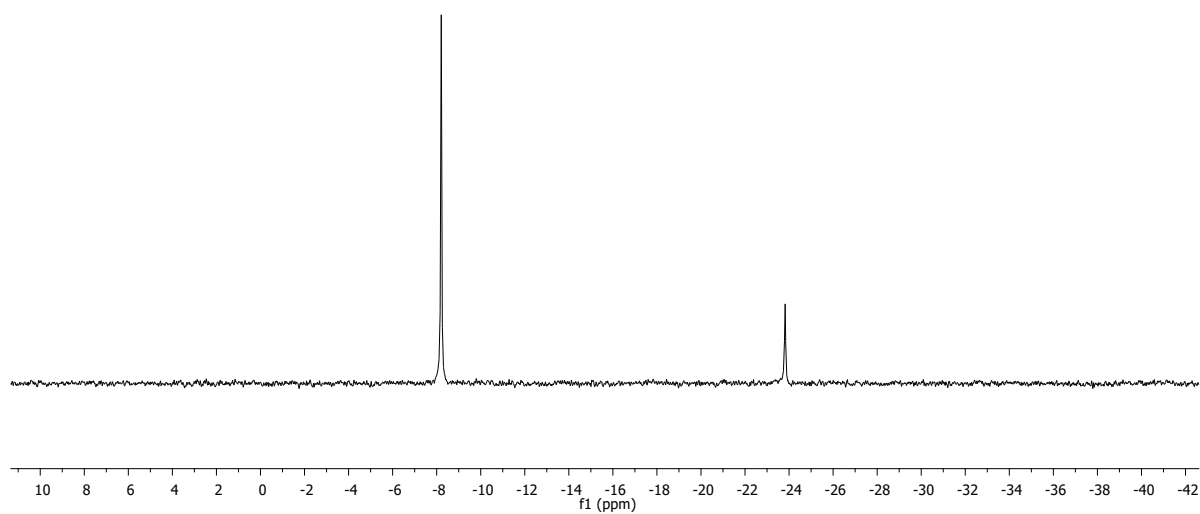
^{1}H NMR of [(Cym)Ru(κ^3P,N,S-H$_2$L1)][SbF$_6$]$_2$ (3) (500.10 MHz, CD$_2$Cl$_2$, RT)
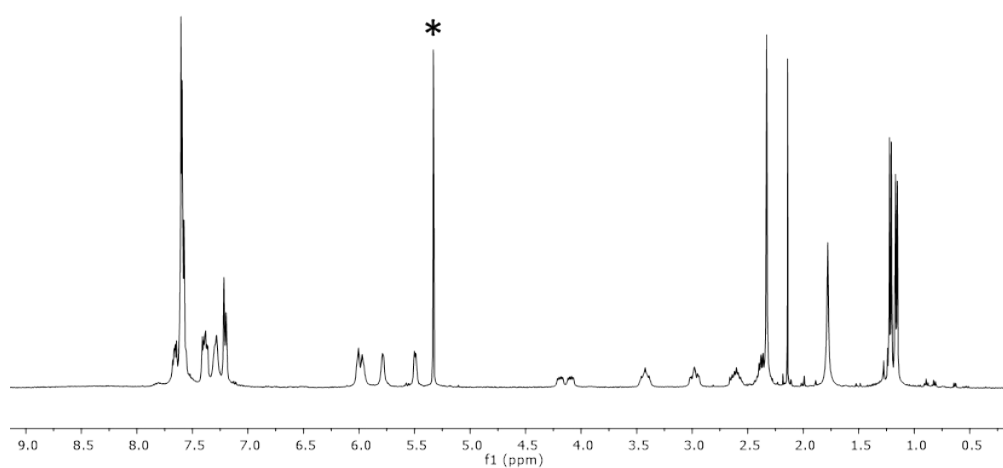
^{13}C{^{1}H} NMR of [(Cym)Ru(κ^3P,N,S-H$_2$L1)][SbF$_6$]$_2$ (3) (125.77 MHz, CD$_2$Cl$_2$, RT)
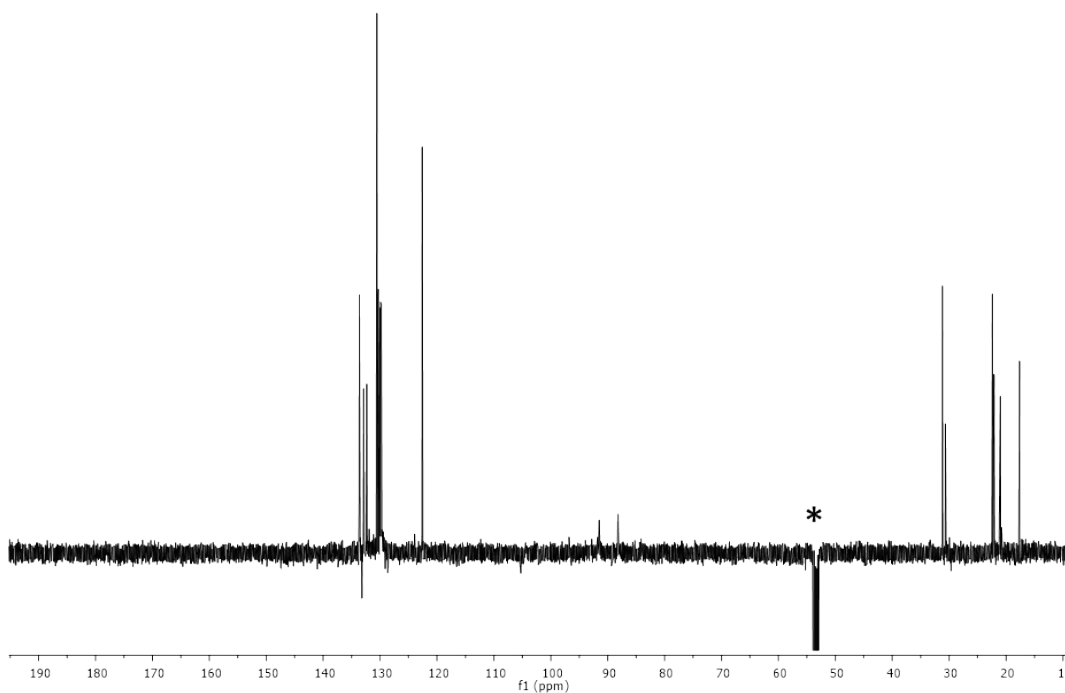
^{31}P{^{1}H} NMR of [(Cym)Ru(κ^3P,N,S-H$_2$L1)][SbF$_6$]$_2$ (3) (202.46 MHz, CD$_2$Cl$_2$, RT)

^{1}H NMR of [(Cym)Os(κ^3P,N,S-H$_2$L1)][SbF$_6$]$_2$ (4) (500.10 MHz, CD$_2$Cl$_2$, RT)

^{13}C{^{1}H} NMR of [(Cym)Os(κ^3P,N,S-H$_2$L1)][SbF$_6$]$_2$ (4) (125.77 MHz, CD$_2$Cl$_2$, RT)
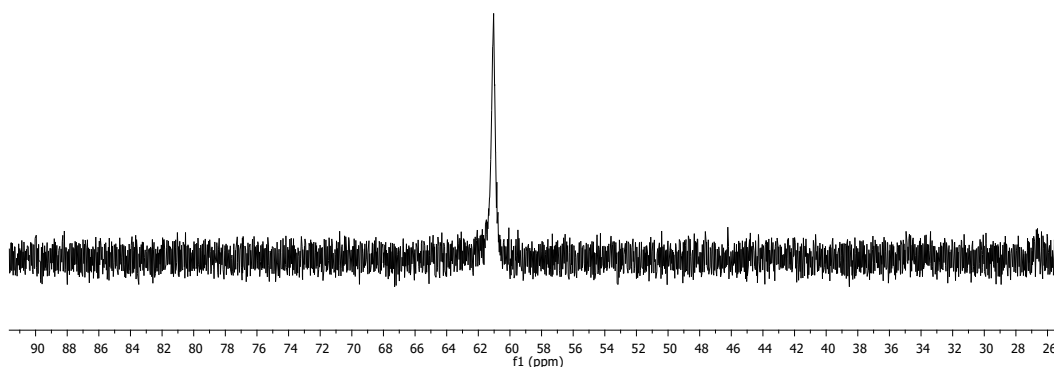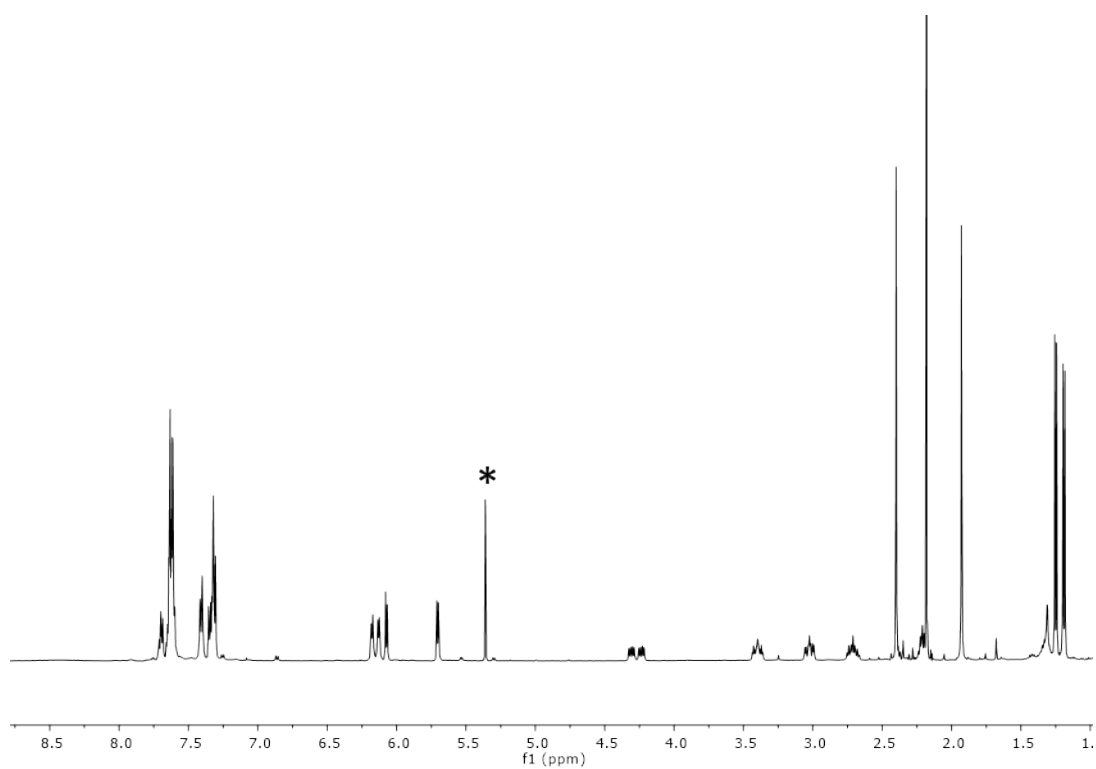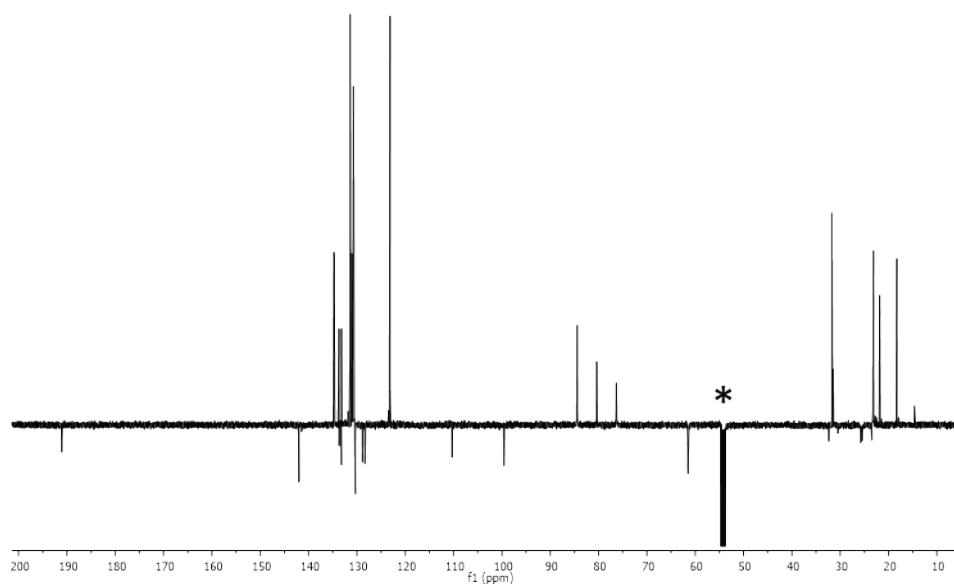
^{31}P{^{1}H} NMR of [(Cym)Os($\kappa^3 P,N,S$-H$_2$L1)][SbF$_6$]$_2$ (4) (202.46 MHz, CD$_2$Cl$_2$, RT)
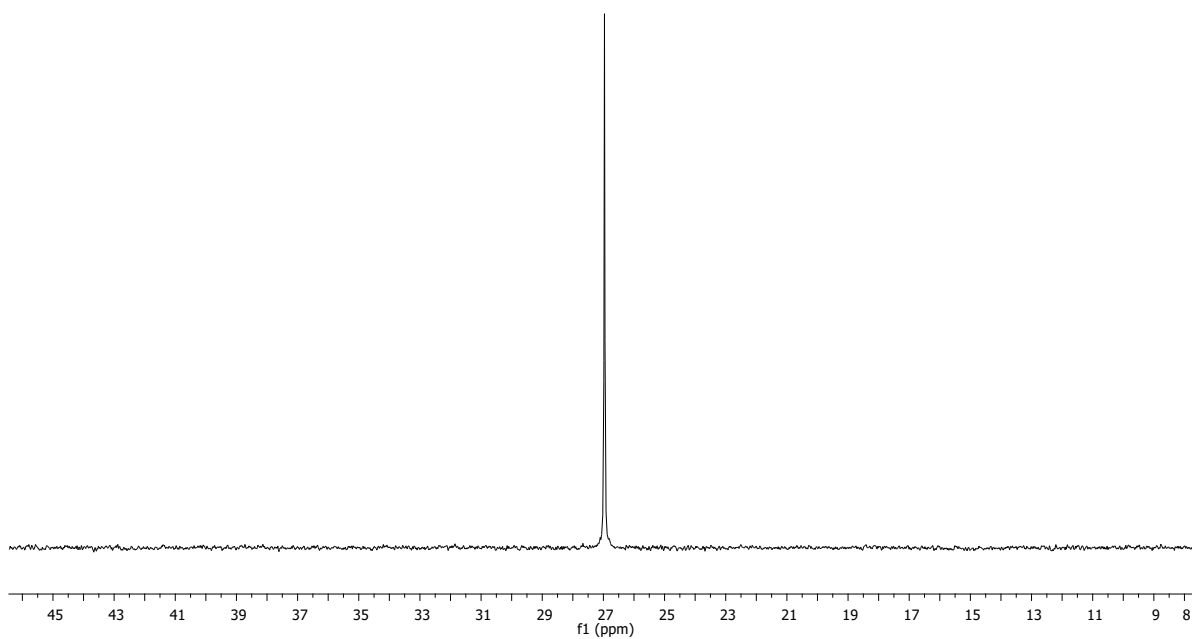
^{1}H NMR of [(Cym)Ru($\kappa^3 P,N,S$-HL1)][SbF$_6$] (5) (500.10 MHz, CD$_2$Cl$_2$, RT)
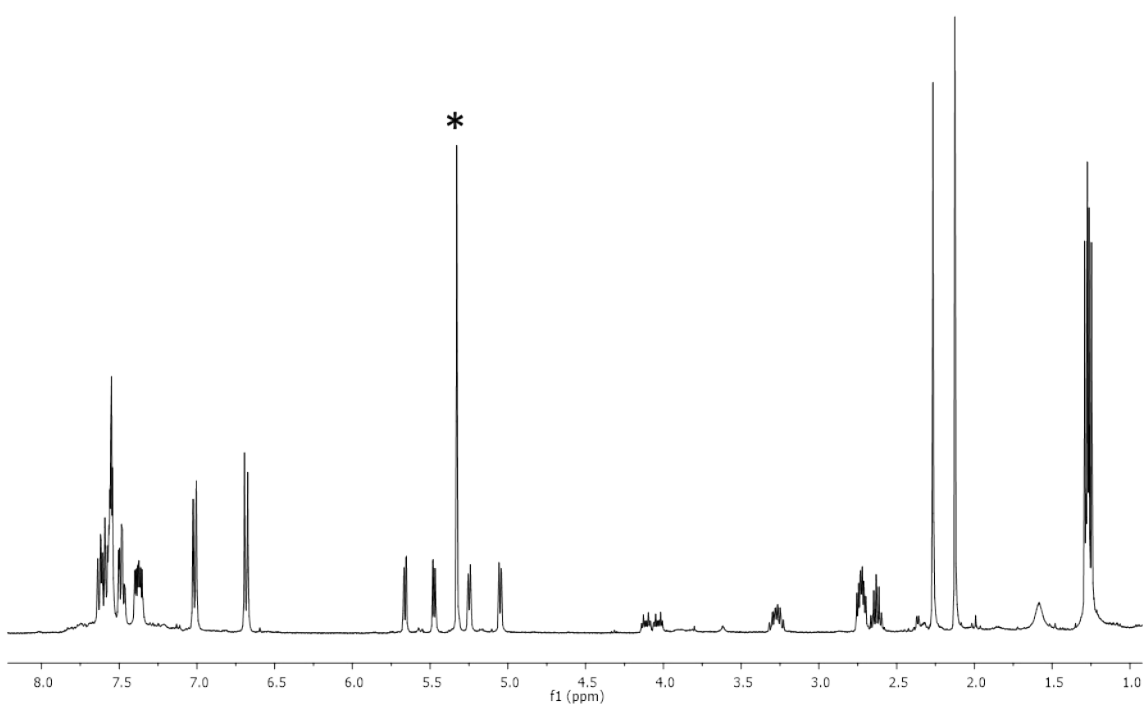
^{13}C{^{1}H} NMR of [(Cym)Ru($\kappa^3 P,N,S$-HL1)][SbF$_6$] (5) (125.77 MHz, CD$_2$Cl$_2$, RT)
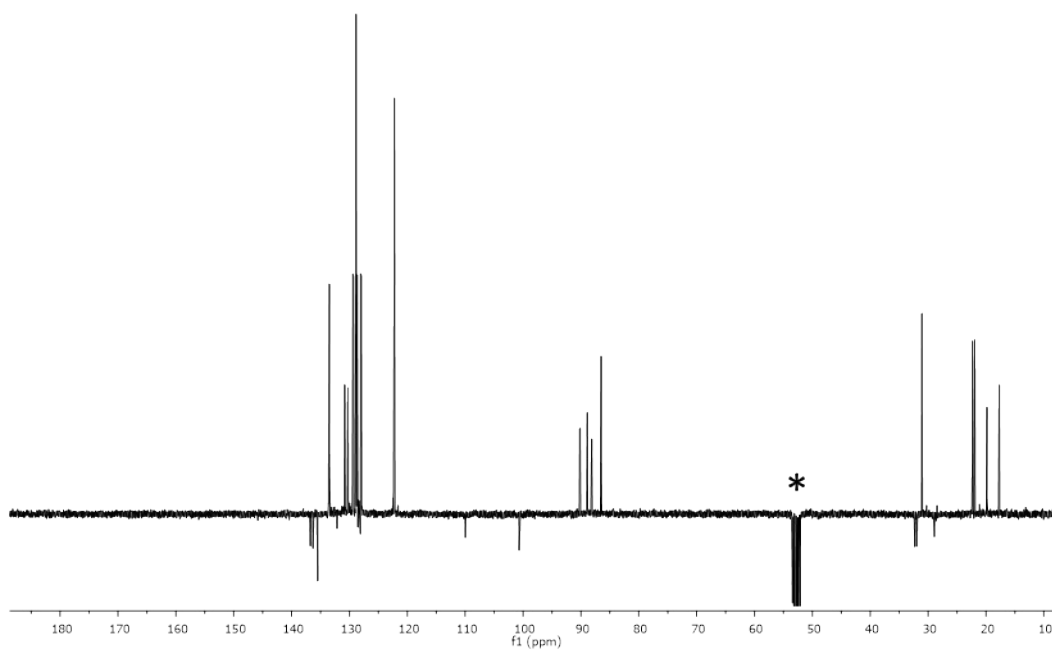
^{31}P{^{1}H} NMR of [(Cym)Ru($\kappa^3 P,N,S$-HL1)][SbF$_6$] (5) (202.46 MHz, CD$_2$Cl$_2$, RT)
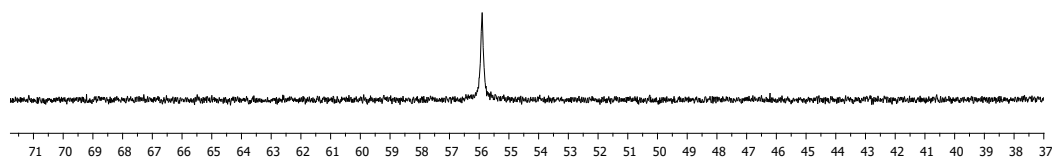
^{31}P{^{1}H} NMR of [(Cym)Ru($\kappa^3 P,N,S$-HL1)][SbF$_6$] (5) (202.46 MHz, CD$_2$Cl$_2$, 173 K)
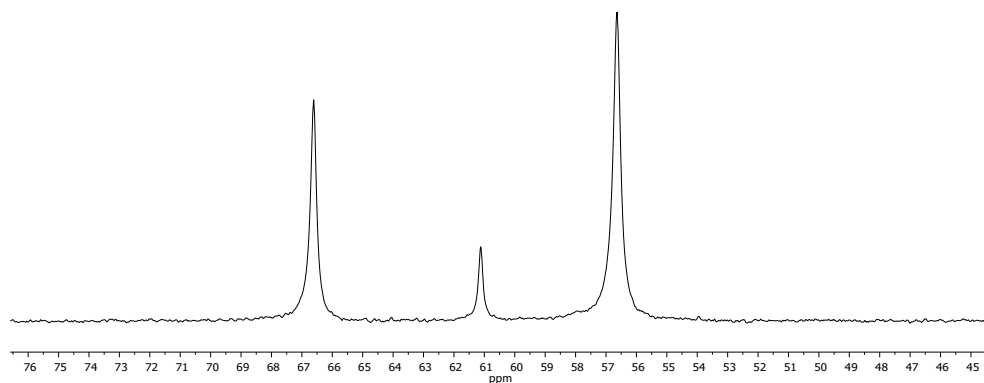
^{1}H NMR of [(Cym)Os(κ^3P,N,S-HL1)][SbF$_6$] (6) (500.10 MHz, CD$_2$Cl$_2$, RT)
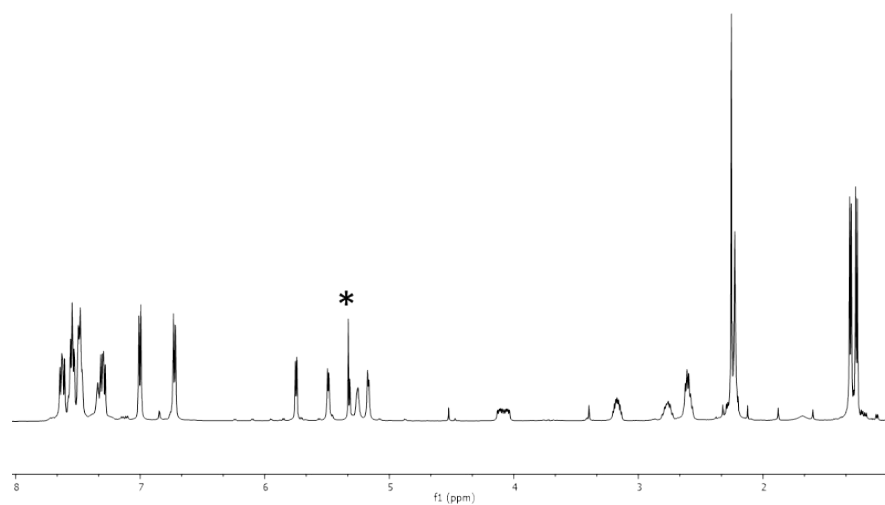
^{13}C{^{1}H} NMR of [(Cym)Os(κ^3P,N,S-HL1)][SbF$_6$] (6) (125.77 MHz, CD$_2$Cl$_2$, RT)
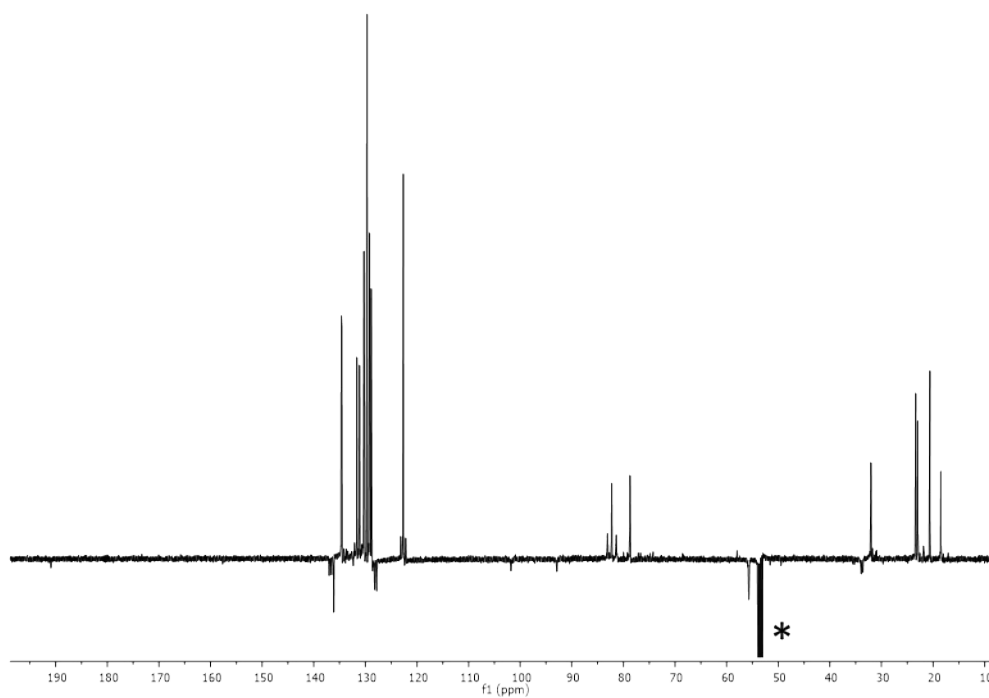
^{31}P{^{1}H} NMR of [(Cym)Os(κ^3P,N,S-HL1)][SbF$_6$] (6) (202.46 MHz, CD$_2$Cl$_2$, RT)
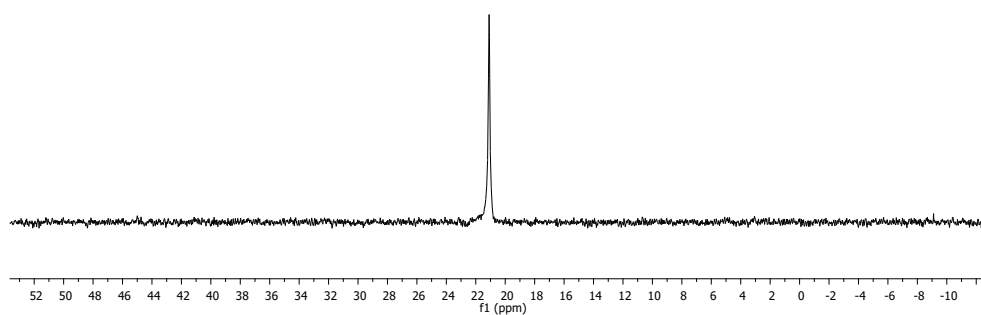
^{31}P{^{1}H} NMR of [(Cym)Os(κ^3P,N,S-HL1)][SbF$_6$] (6) (202.46 MHz, CD$_2$Cl$_2$, 173 K)
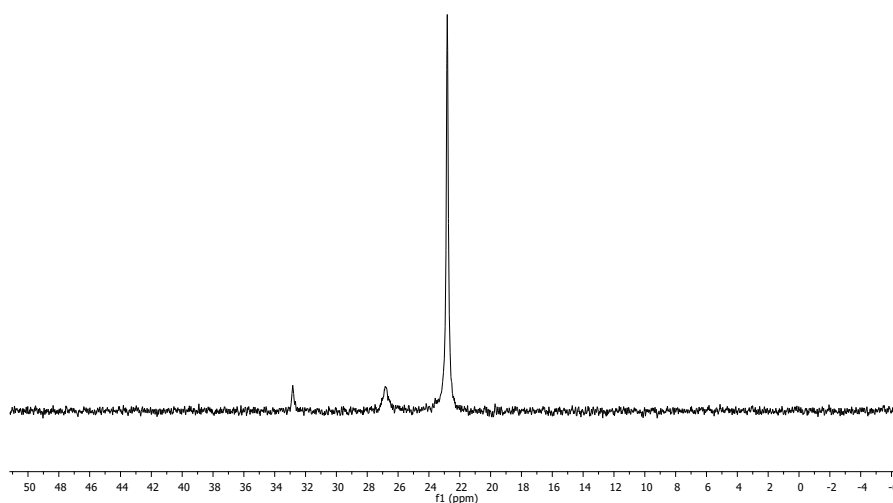
^{1}H NMR of [(Cym)RuH(κ^2P,S-H$_2$L1)][SbF$_6$] (11) (500.10 MHz, THF-d_8, RT)
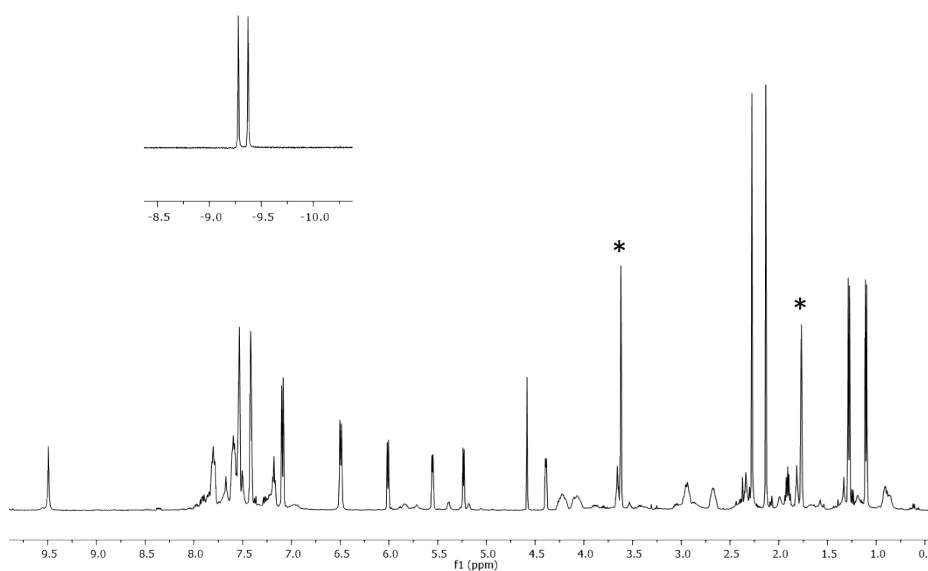
^{13}C{^{1}H} NMR of [(Cym)RuH(κ^2P,S-H$_2$L1)][SbF$_6$] (11) (125.77 MHz, THF-d_8, RT)
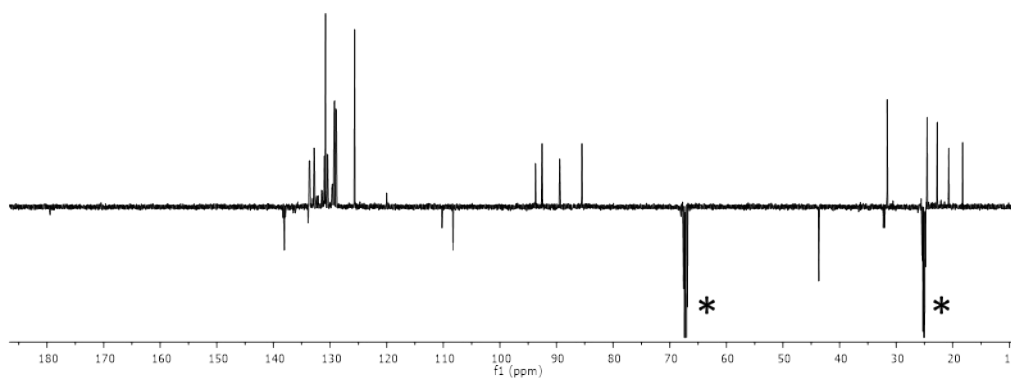
^{31}P{^{1}H} NMR of [(Cym)RuH(κ^{2}P,S-H$_2$L1)][SbF$_6$]$_2$ (11) (202.46 MHz, THF-d_8, RT)
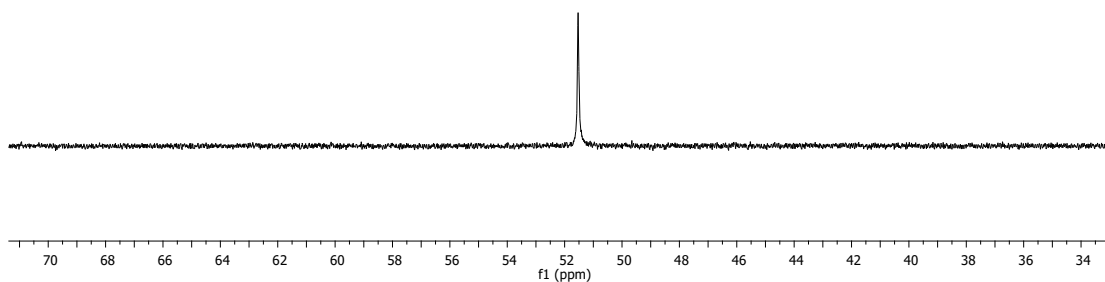
^{31}P{^{1}H} NMR of [(Cym)RuH(κ^{2}P,S-H$_2$L1)][SbF$_6$] (11) (202.46 MHz, THF-d_8, 173K)
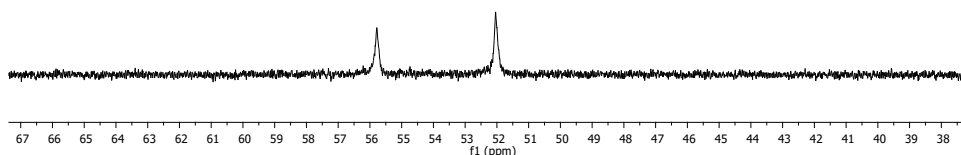
^{1}H NMR of [(Cym)OsH(κ^{2}P,S-H$_2$L1)][SbF$_6$] (12) (500.10 MHz, THF-d_8, RT)
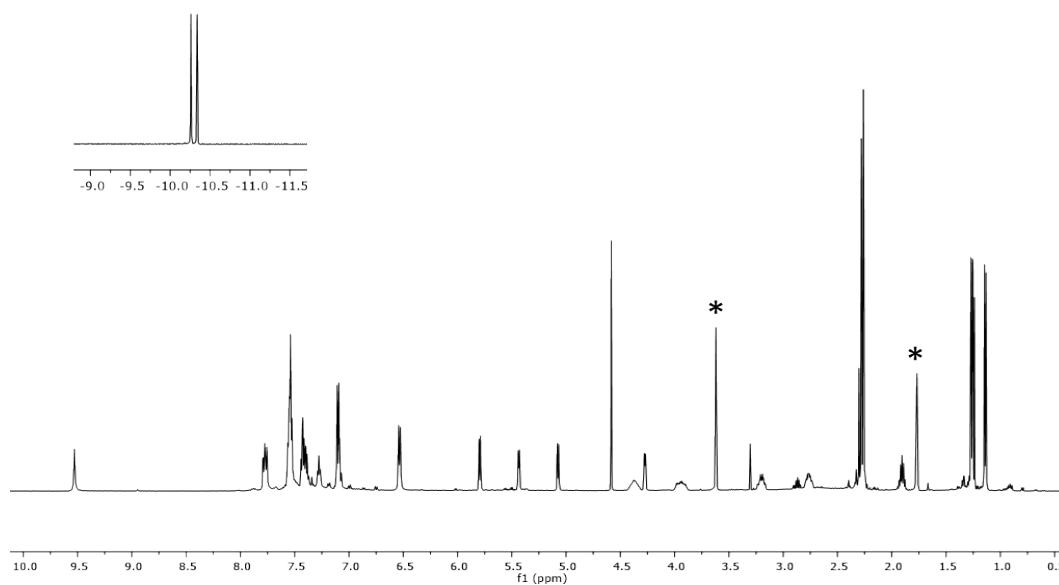
^{13}C{^{1}H} NMR of [(Cym)OsH($\kappa^2 P,S$-H$_2$L1)][SbF$_6$] (12) (125.77 MHz, THF-d_8, RT)
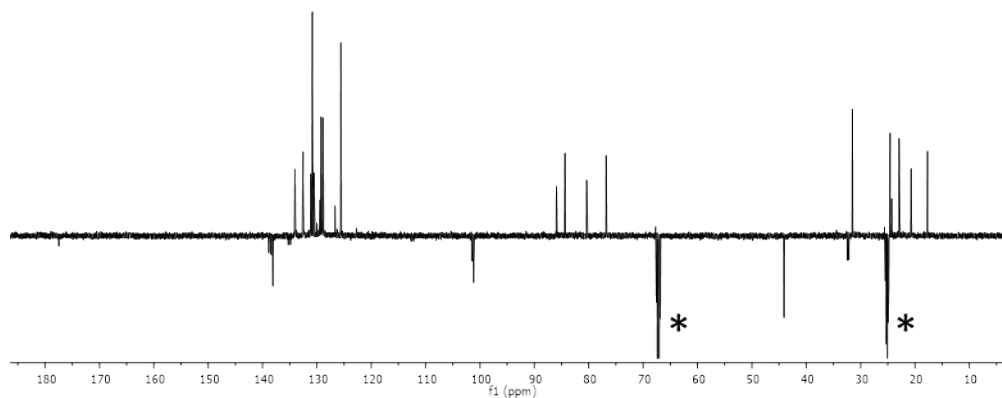
^{31}P{^{1}H} NMR of [(Cym)OsH($\kappa^2 P,S$-H$_2$L1)][SbF$_6$]$_2$ (12) (202.46 MHz, THF-d_8, RT)
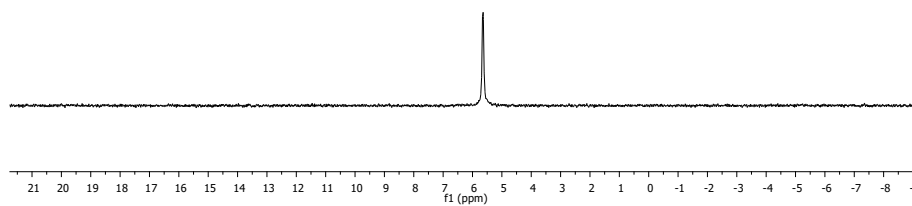
^{31}P{^{1}H} NMR of [(Cym)OsH($\kappa^2 P,S$-H$_2$L1)][SbF$_6$]$_2$ (12) (202.46 MHz, THF-d_8, 193K)
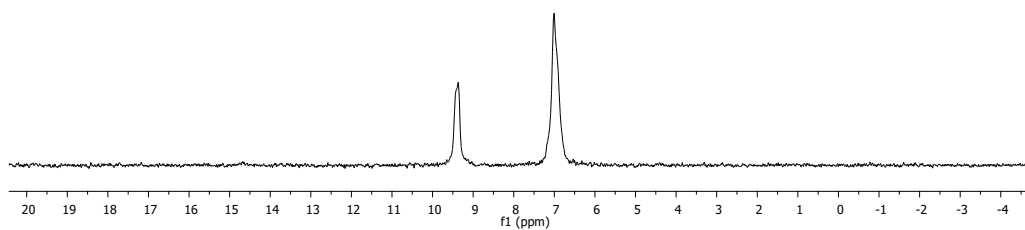
¹H NMR of [(Cym)RuH(κ²*P*,*N*-H₂L2)][SbF₆] (13) (500.10 MHz, THF-*d₈*, RT)
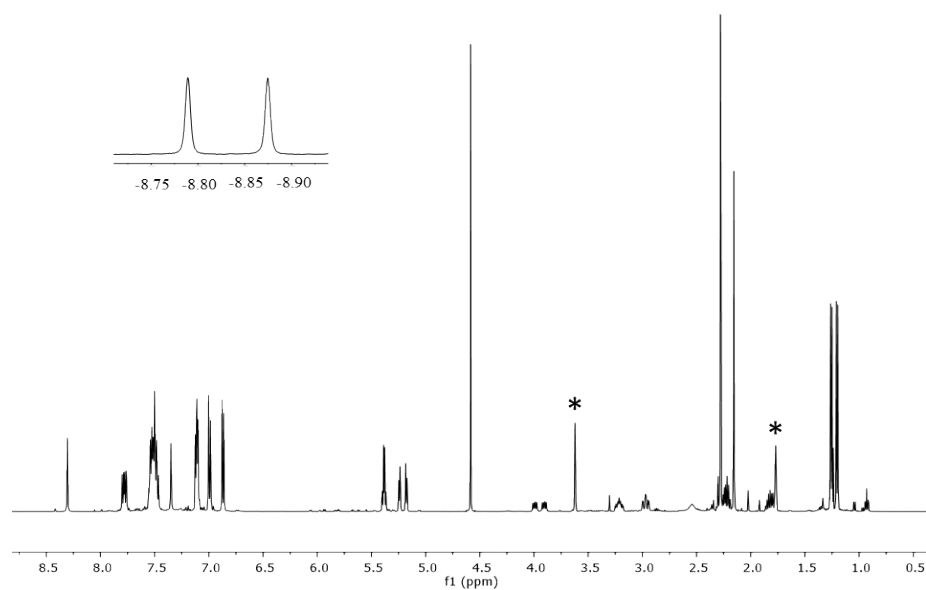
¹³C{¹H} NMR of [(Cym)RuH(κ²*P*,*N*-H₂L2)][SbF₆] (13) (125.77 MHz, THF-*d₈*, RT)
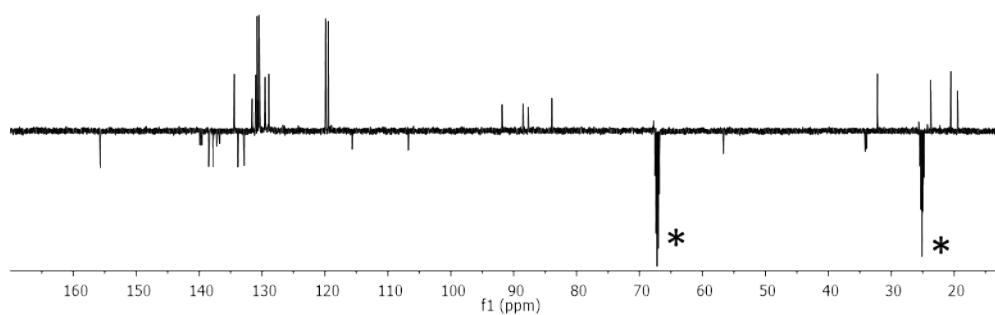
³¹P{¹H} NMR of [(Cym)RuH(κ²*P*,*N*-H₂L2)][SbF₆]₂ (13) (202.46 MHz, THF-*d₈*, RT)
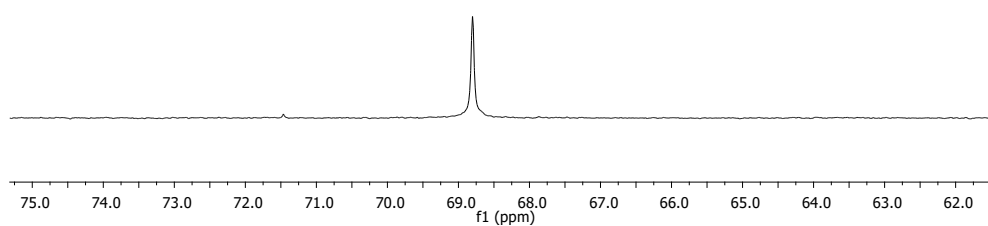
¹H NMR of [(Cym)OsH(κ²*P*,*N*-H₂L2)][SbF₆] (14) (500.10 MHz, CD₂Cl₂, RT)
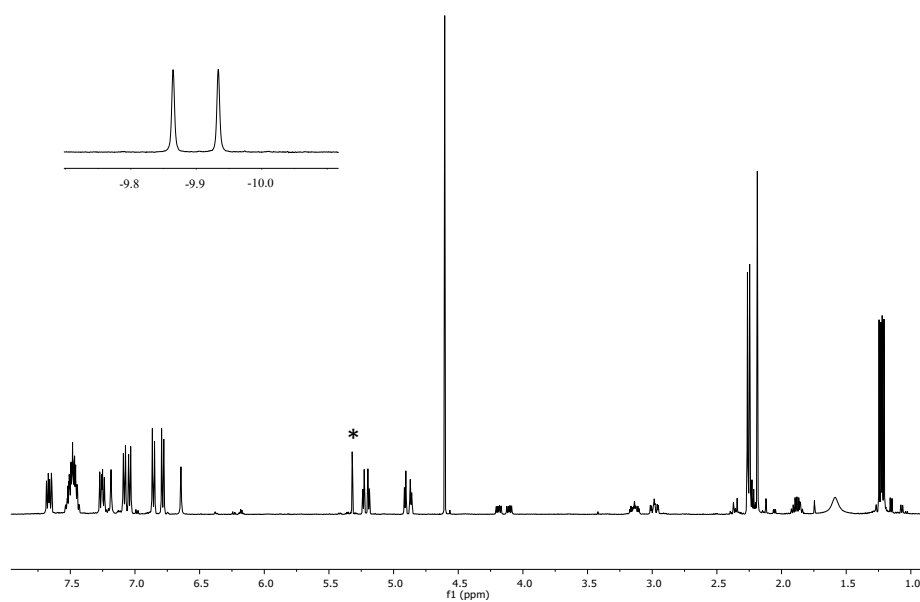
¹³C{¹H} NMR of [(Cym)OsH(κ²*P*,*N*-H₂L2)][SbF₆] (14) (125.77 MHz, CD₂Cl₂, RT)
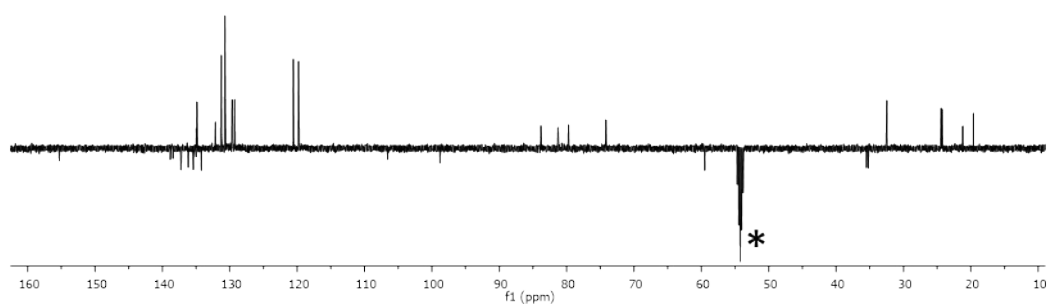
³¹P{¹H} NMR of [(Cym)OsH(κ²*P*,*N*-H₂L2)][SbF₆]₂ (14) (202.46 MHz, CD₂Cl₂, RT)
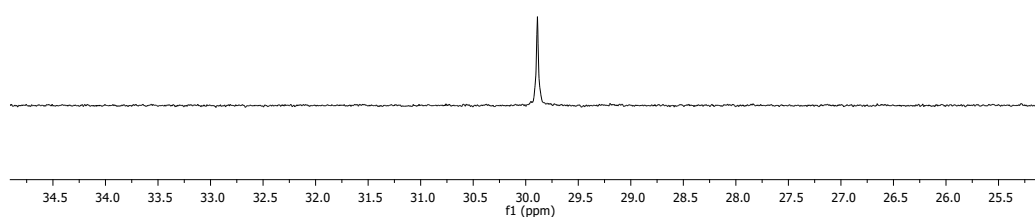
173 K
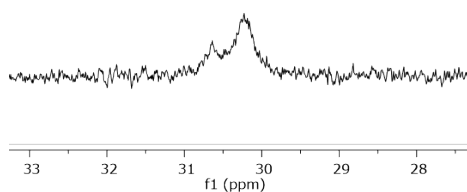
¹H NMR of [(Cym)RuH(κ²N,N'-H₂L3)][SbF₆] (15) (500.10 MHz, THF-*d₈*, RT)
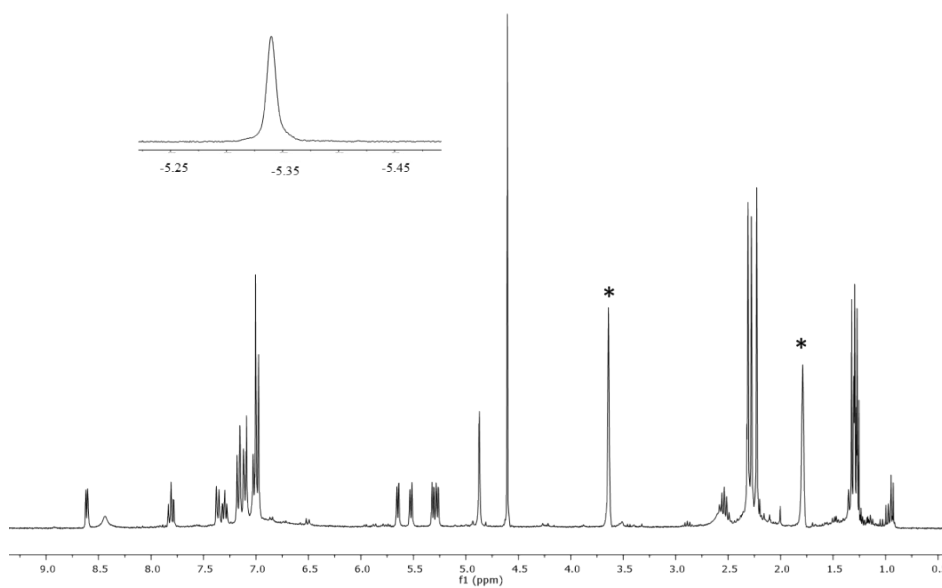
¹³C{¹H} NMR of [(Cym)RuH(κ²N,N'-H₂L3)][SbF₆] (15) (125.77 MHz, THF-*d₈*, RT)
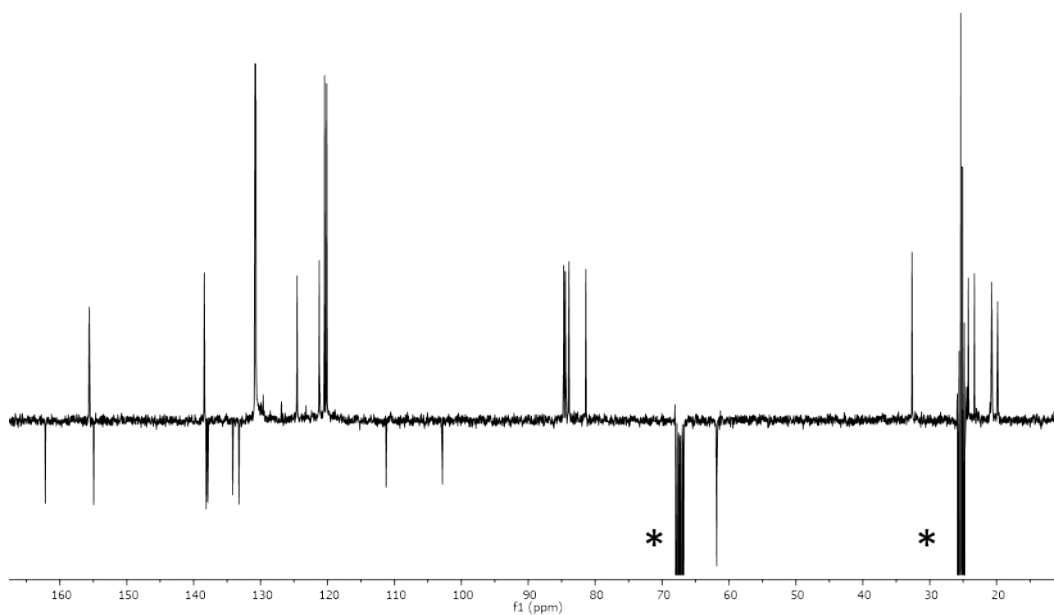
¹H NMR of [(Cym)OsH(κ²*N,N'*-H₂L3)][SbF₆] (16) (500.10 MHz, THF-*d₈*, RT)
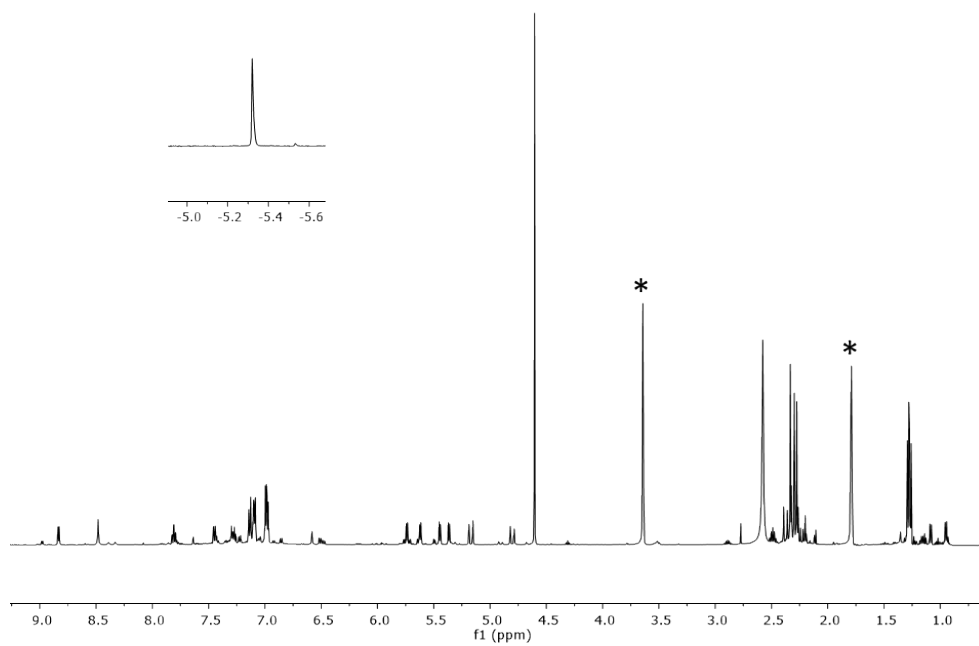
¹³C{¹H} NMR of [(Cym)OsH(κ²*N,N'*-H₂L3)][SbF₆] (16) (125.77 MHz, THF-*d₈*, RT)
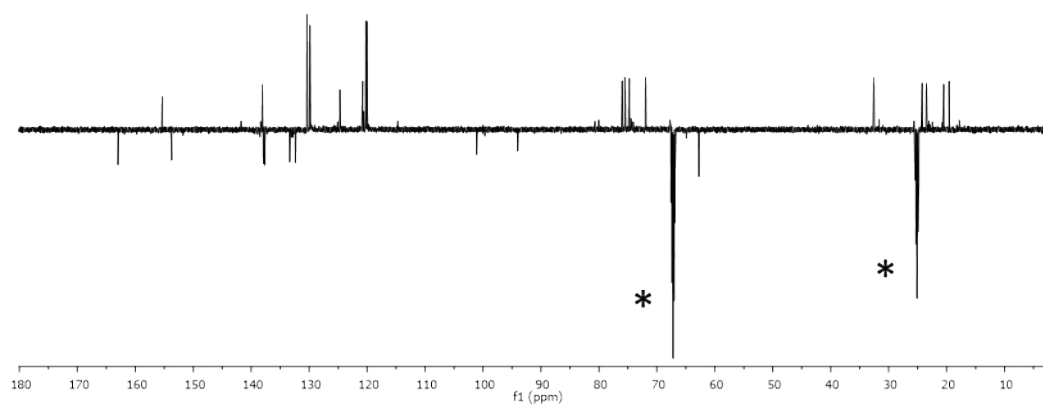
¹H NMR of [(Cym)Ru(κ³*N*,*N'*,*C*-H₂L3₋ₕ)][SbF₆] (17) (500.10 MHz, CD₃OD, RT)
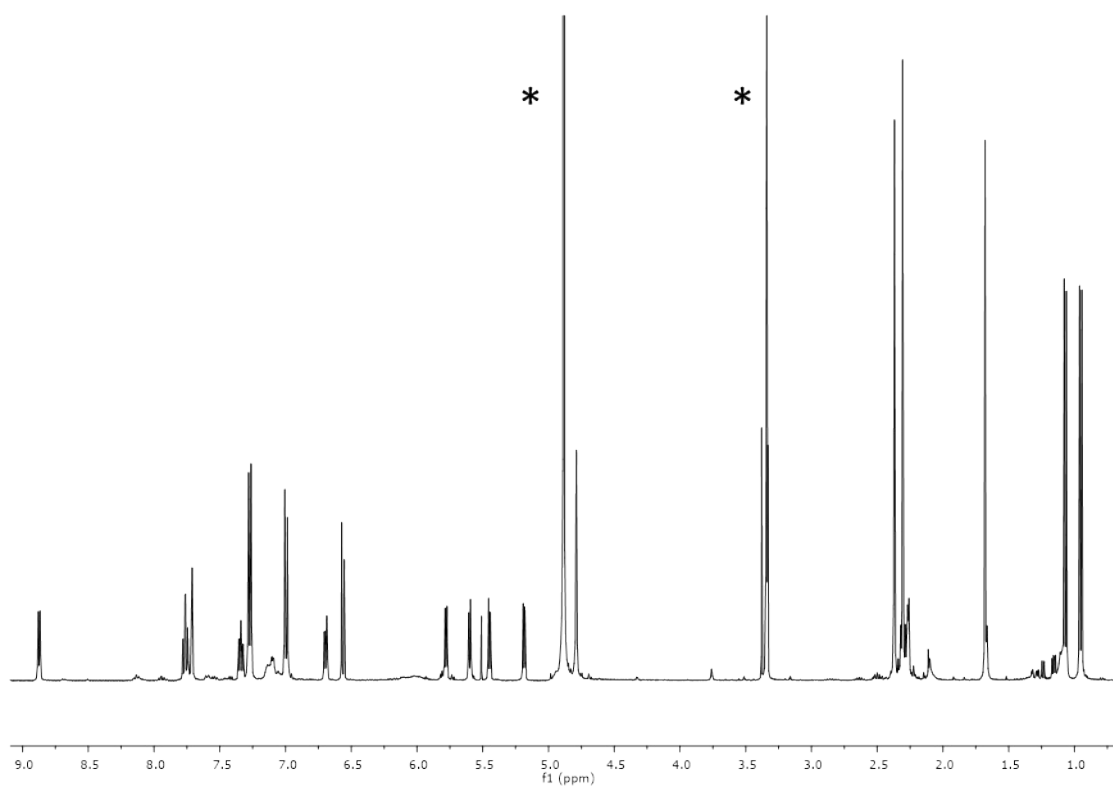
¹³C{¹H} NMR of [(Cym)Ru(κ³*N*,*N'*,*C*-H₂L3₋ₕ)][SbF₆] (17) (125.77 MHz, CD₃OD, RT)
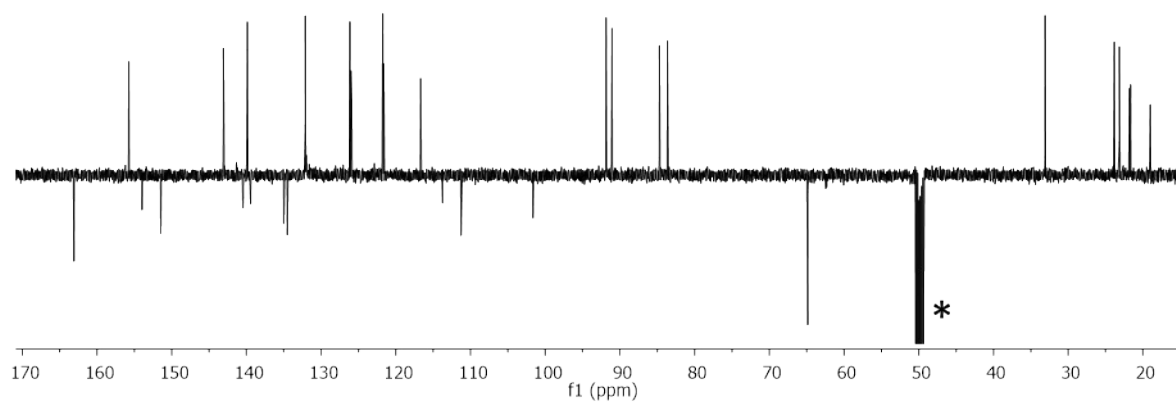
^{1}H NMR of [(Cym)Os(κ^3*N,N',C*-H$_2$L3$_{-H}$)][SbF$_6$] (18) (500.10 MHz, CD$_3$OD, RT)
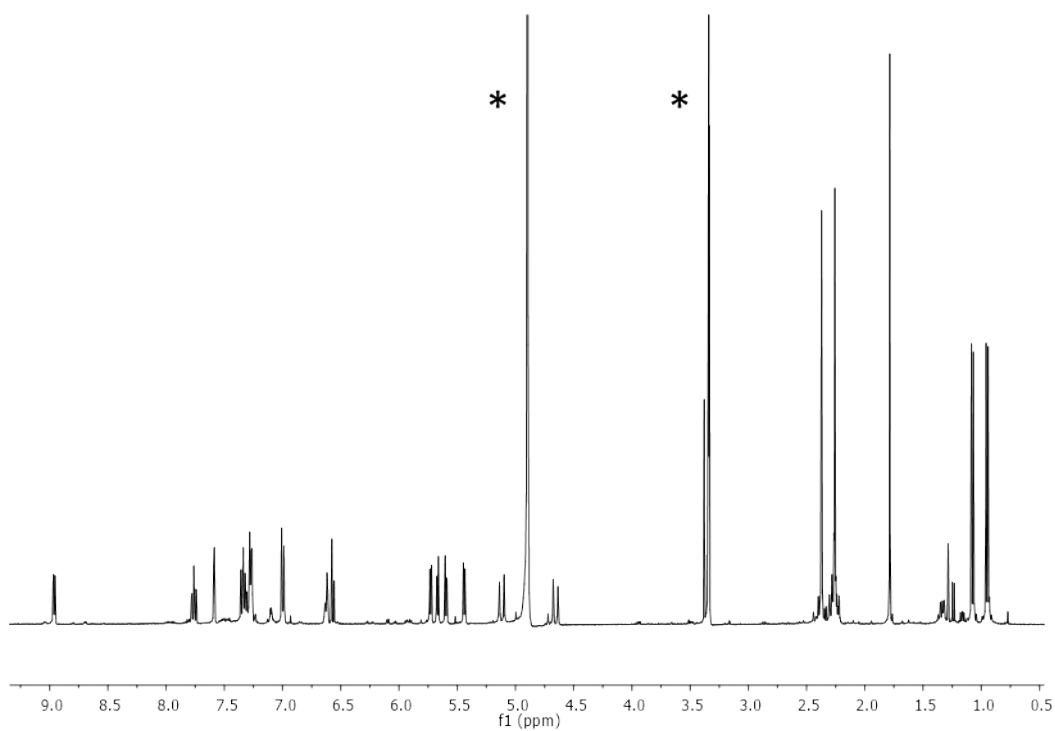
^{13}C{^{1}H} NMR of [(Cym)Os(κ^3*N,N',C*-H$_2$L3$_{-H}$)][SbF$_6$] (18) (125.77 MHz, CD$_3$OD, RT)
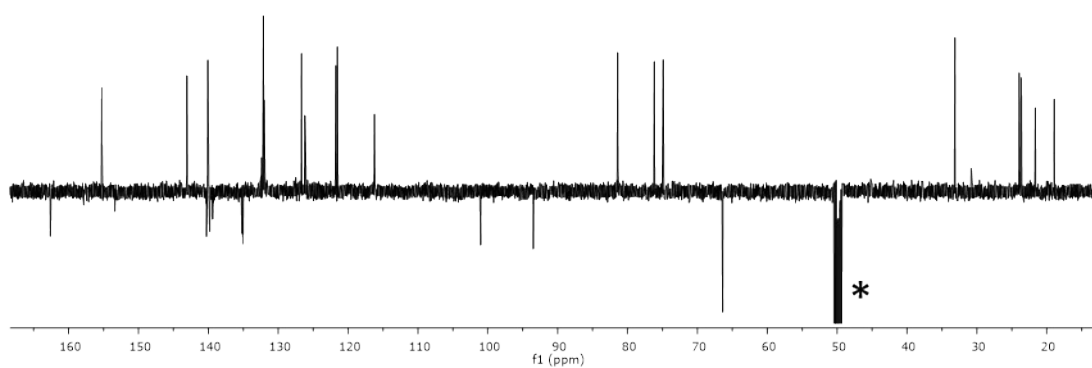
¹H NMR of complex 19 (500.10 MHz, THF-*d₈*, RT)

Isolated from the catalytic hydrogenation
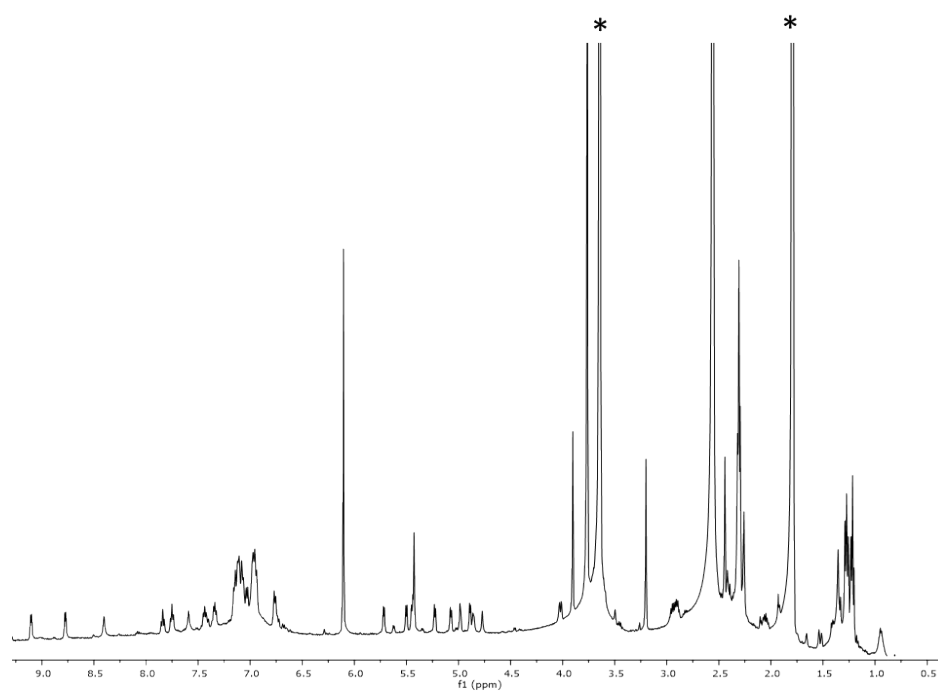
¹H NMR of 19 (500.10 MHz, CD₂Cl₂, RT)

Prepared from complex **9** and methyl acrylate
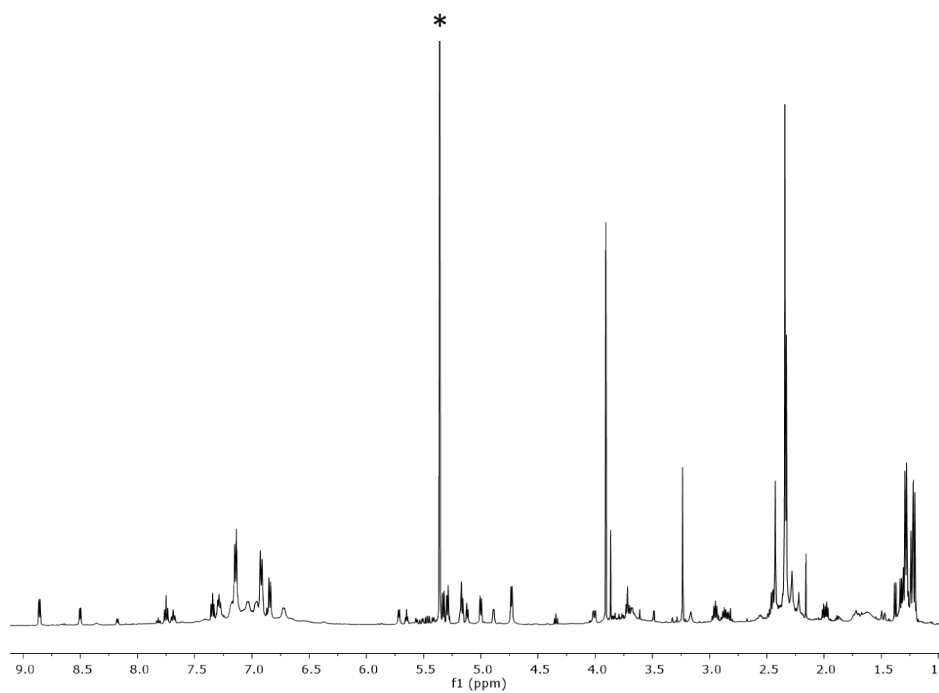
$^{13}C\{^1H\}$ of complex 19 (500.10 MHz, CD$_2$Cl$_2$, RT)
Prepared from complex **9** and methyl acrylate
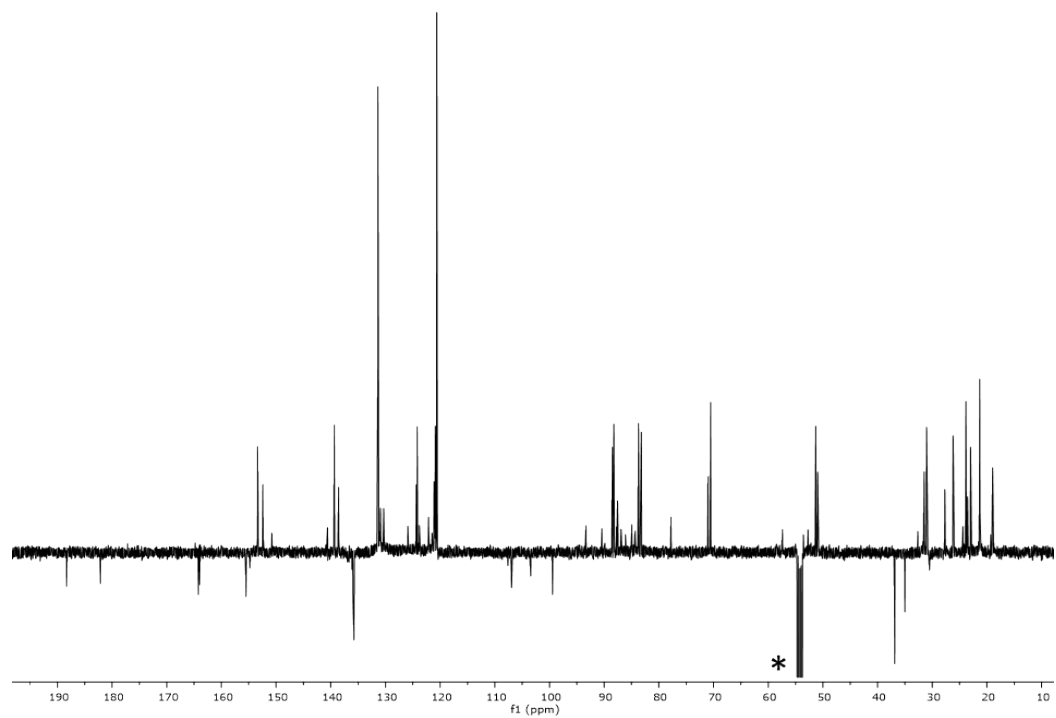
6 Catalytic hydrogenation essays

Table S1 Hydrogenation of methyl acrylate[a]
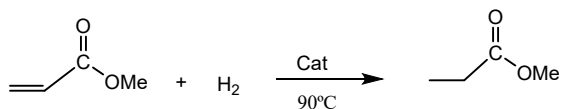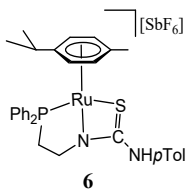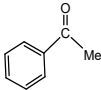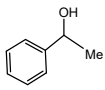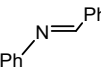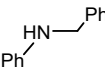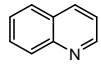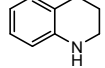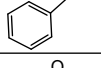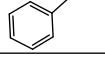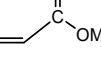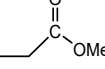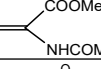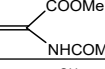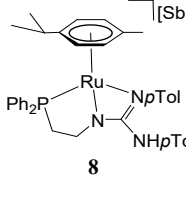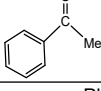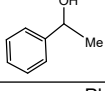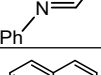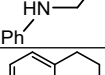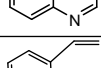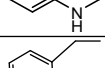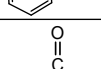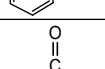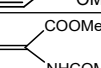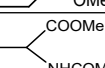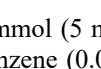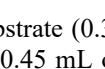
Entry	Catalyst	t (h)	Conv. (%)[b]
1	**6**	7	100
2	**7**	30	91
3	**8**	7	100
4	**9**	216	71
5	**10**	8	99
6	**11**	216	72

[a]Reaction conditions: catalyst 0.015 mmol (5 mol %), methyl acrylate (0.30 mmol), H_2 (5 bar), internal reference 1,3,5-trimethoxybenzene (0.03 mol), in 0.45 mL of THF-d[8]. [b]Based on 1,3,5-trimethoxybenzene. Determined by NMR.

Table S2 Hydrogenation of unsatutared substrates[a]

$$R^1\text{--}X{=}C(R^2)R^3 + H_2 \xrightarrow[90°C]{\text{Cat}} R^1\text{--}X(H)\text{--}C(H)(R^2)R^3$$
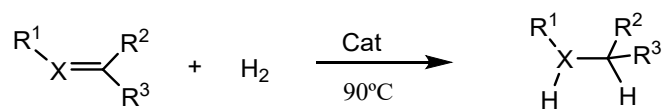
Entry	Catalyst	Substrate	Product	t(h)	Conv. (%)[b]
1	catalyst **6** ([SbF₆], Ru, Ph₂P, S, N, C, NHpTol)	acetophenone (C₆H₅COMe)	1-phenylethanol (C₆H₅CH(OH)Me)	72	3
2		PhN=CHPh	PhNH–CH₂Ph	24	99
3		quinoline	1,2,3,4-tetrahydroquinoline	24	100
4		styrene	ethylbenzene	96	87
5		methyl acrylate (CH₂=CH–COOMe)	methyl propanoate	7	100
6		CH₂=C(COOMe)(NHCOMe)	CH₂=C(COOMe)(NHCOMe)	14	100
7	catalyst **8** ([SbF₆], Ru, Ph₂P, NpTol, N, NHpTol)	acetophenone (C₆H₅COMe)	1-phenylethanol (C₆H₅CH(OH)Me)	72	100
8		PhN=CHPh	PhNH–CH₂Ph	29	97
9		quinoline	1,2,3,4-tetrahydroquinoline	96	94
10		styrene	ethylbenzene	67	93
11		methyl acrylate (CH₂=CH–COOMe)	methyl propanoate	7	100
12		CH₂=C(COOMe)(NHCOMe)	CH₃CH(COOMe)(NHCOMe)	55	100

[a]Reaction conditions: catalyst 0.015 mmol (5 mol %), substrate (0.30 mmol), H₂ (5 bar), internal reference 1,3,5-trimethoxybenzene (0.03 mol) in 0.45 mL of THF-d⁸. [b]Based on 1,3,5-trimethoxybenzene. Determined by NMR.

Table S3 Hydrogenation of acrylates[a]
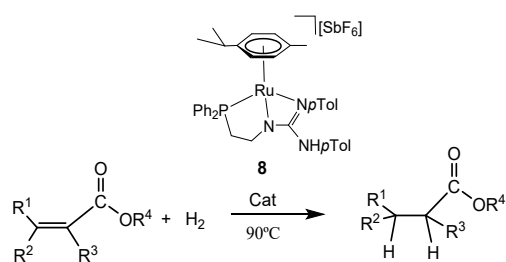
Entry	Catalyst (mol%)	Substrate	Product	t	Conv. (%)[b]
1	5	(methyl acrylate)	(methyl propanoate, OMe)	7	100
2[c]	1			30	100
3[d]	1			26	100
4[e]	0.1			116	91
5	5	(ethyl acrylate, OEt)	(OEt)	10	98
6	5	(OtBu)	(OtBu)	5	100
7	5	(O–CH₂CF₃)	(O–CH₂CF₃)	5	100
8	5	(methyl methacrylate, OMe)	(OMe)	72	90
9	5	(ethyl crotonate, OEt)	(OEt)	45	67
10	5	(methyl 3-methyl-2-butenoate, OMe)	(OMe)	144	14

[a]Reaction conditions: catalyst 0.015 mmol (5 mol %), substrate (0.30 mmol), H$_2$ (5 bar), internal reference 1,3,5-trimethoxybenzene (0.03 mol), in 0.45 mL of THF-d^8. [b]Based on 1,3,5-trimethoxybenzene. Determined by NMR. [c]Catalyst 0.003 mmol (1 mol %), methyl acrylate (0.30 mmol). [d]Catalyst 0.003 mmol (1 mol %), methyl acrylate (0.30 mmol) in 0.45 mL of D$_2$O. [e]Catalyst 0.0015 mmol (0.1 mol %), methyl acrylate (1.50 mmol) in 0.45 mL of D$_2$O.

7 X-ray crystallography

X-ray diffraction data were collected on a Smart APEX (**4**, **6**), APEX DUO (**2**, **5**, **17**) or D8 VENTURE (**13**, **19**) Bruker diffractometers, using graphite-monochromated Mo κα radiation (λ = 0.71073 Å). Single crystals were mounted on a fiber or a micromount, coated with a protecting perfluoropolyether oil and cooled to 100(2) K (complexes **2** ,**4, 5**, **13**, **17**, **19**) or 150 K (compound **7**) with an open-flow nitrogen gas. Data were collected using ω-scans (and φ-scans for **13** and **19**) and narrow oscillation frame strategies. Diffracted intensities were integrated and corrected for absorption effects by using multi-scan method using SAINT[S2] and SADABS[S3] programs, included in APEX2 or APEX4 (for **13** and **19**) packages. Structures were solved by Patterson or direct methods with SHELXS[S4] and refined by full-matrix least squares on F^2 with SHELXL program[S5] included in Wingx program system[S6] or OLEX2 program.[S7] Although hydrogen atoms have been observed in Fourier difference maps, most of them have been included in the model in calculated positions and refined with a riding model. The NH hydrogen atoms have been included in calculated positions and refined with a riding model (complexes **4, 5**, **13**, **14** and **19**), or included in observed positions, and refined with geometrical restrains in N-H bond lengths (compound **17**) with isotropic displacement parameters restrained to be 1.2 times the Ueq of their N parent atoms (compound **2** and **6**). The presence of hydride ligand in isostructural **13** and **14** has been evidenced by NMR of the crystals of complex **14**. Hydride positions have been determined with HYDEX program[S8] and kept fixed. Further details about specific problems encountered in data reduction or structure refinement (disorder or solvent modelling) are described below.

Structural data for *2*: $C_{32}H_{37}ClF_6N_2OsPSSb$; M_r = 974.06; orange prism, 0.075 × 0.085 × 0.150 mm³; triclinic $P\bar{1}$; a = 10.3781(9) Å, b = 10.4833(9) Å, c = 16.9677(15) Å; α = 97.1740(10)º, β = 103.529(2)º, γ = 99.2620(10)º ; V = 1745.8(3) Å³, Z = 2, D_c = 1.853 g/cm³; μ = 4.649 cm⁻¹; min. and max. absorption correction factors: 0.590 and 0.845, $2\theta_{max}$ = 60.494°;

17326 reflections measured, 8271 unique; R_{int} = 0.0549; number of data/restraint/parameters 8271/2/416; R_1 = 0.0371 [6087 ref. with $I > 2\sigma(I)$], w$R(F^2)$ = 0.0706 (all data); largest difference peak 1.918 e·Å^{-3}. During the data collection the crystal fell from the top of the glass fiber. Another crystal was mounted and therefore two sets of data were then measured. Both were corrected from absoprtion and scale with SORTAV program.[S9] The sample forms prismatic crystals mutually stuck and weakly diffracting. Selected crystals were selected as indexation processes were successful. However, at the end of the data treatment completeness was not achieved for this triclinic structure.

Structural data for 4: $C_{32}H_{36}F_{12}N_2OsPSSb_2 \cdot C_6H_{14} \cdot 5(H_2O) \cdot 0.5(CH_2Cl_2)$; Mr = 1371.11; yellow plate, 0.070 × 0.095 × 0.150 mm^3; triclinic $P\bar{1}$; a = 10.1759(6) Å, b = 15.2630(8) Å, c = 15.4343(8) Å; α = 86.7350(10)^o, β = 80.2470(10)^o, γ = 81.2590(10)^o ; V = 2333.9(2) Å^3, Z = 2, Dc = 1.951 g/cm^3; μ = 4.087 cm^{-1}; min. and max. absorption correction factors: 0.5885 and 0.7278, 2θmax = 56.952°; 26736 reflections measured, 10801 unique; $Rint$ = 0.0443; number of data/restraint/parameters 10801/0/473; $R1$ = 0.0503 [8824 ref. with $I > 2\sigma(I)$], w$R(F2)$ = 0.1013 (all data); largest difference peak 1.720 e·Å^{-3}. Asymmetric unit contains solvent, including a water molecule interacting with a NH fragment. The rest of the solvent has been found to be highly disordered, its inclusion in the structural model leads to unrealistic geometrical parameters. The contribution of this solvent to diffracted intensity has been calculated with a solvent mask.

Structural data for 5: $C_{32}H_{36}F_6N_2PRuSSb \cdot CH_4O$; Mr = 880.54; yellow prism, 0.140 × 0.150 × 0.150 mm^3; monoclinic $P2_1/n$; a = 9.0786(5) Å, b = 21.1970(12) Å, c = 18.2541(10) Å; β = 97.1700(10)^o ; V = 3485.3(3) Å^3, Z = 4, Dc = 1.686 g/cm^3; μ = 1.374 cm^{-1}; min. and max. absorption correction factors: 0.8074 and 0.8620, 2θmax = 52.182°; 46641 reflections measured, 7072 unique; $Rint$ = 0.0332; number of data/restraint/parameters 7072/13/388; $R1$ = 0.0638 [5829 ref. with $I > 2\sigma(I)$], w$R(F2)$ = 0.1604 (all data); largest difference peak 3.514 e·Å^{-}

[3]. A dynamic disordered has been observed in four fluorine atoms of the counterion. It has been modelled with three sets of positions, and refined with geometrical restraints and a common isotropic displacement parameter. Furthermore, *p*-cymene and part of tridentate ligand have been found to be disordered. Involved atoms have been included in the model in two sets of positions with complementary occupancy factors.

Some unsuccessful tests have been performed in order to model residual density peaks as solvent. Solvent contribution to calculated structure factors has been calculated with a solvent mask procedure included in OLEX2.

Structural data for 6: $C_{32}H_{36}F_6N_2POsSSb \cdot 0.5(C_5H_{12})$; $Mr = 973.68$; yellow needle, $0.060 \times 0.070 \times 0.300$ mm^3; monoclinic $P2_1/n$; $a = 9.1041(8)$ Å, $b = 21.3312(16)$ Å, $c = 18.2996(14)$ Å; $\beta = 96.8650(10)^{\circ}$; $V = 3528.3(5)$ Å^3, $Z = 4$, $Dc = 1.833$ g/cm^3; $\mu = 4.527$ cm^{-1}; min. and max. absorption correction factors: 0.4637 and 0.6257, 2θmax $= 56.568°$; 23365 reflections measured, 8078 unique; $Rint = 0.0719$; number of data/restraint/parameters 8078/7/398; $R1 = 0.0751$ [5272 ref. with $I > 2\sigma(I)$], $wR(F2) = 0.1643$ (all data); largest difference peak 1.539 e·Å^{-3}. A dynamic disordered has been observed in four fluorine atoms of the counterion. It has been modelled with two sets of positions, and isotropically refined. Some unsuccessful tests have been performed in order to model residual density peaks as solvent (pentane). Solvent contribution to calculated structure factors has been calculated with SQUEEZE program.[S10]

Structural data for 13: $C_{39}H_{44.93}Cl_{0.07}F_6N_3PRuSb \cdot C_{39}H_{44.96}Cl_{0.04}F_6N_3PRuSb$; $Mr = 1851.01$; yellow prism, $0.066 \times 0.080 \times 0.180$ mm^3; monoclinic $P2_1/c$; $a = 27.2956(12)$ Å, $b = 11.7168(5)$ Å, $c = 24.4621(11)$ Å; $\beta = 92.768(2)^{\circ}$; $V = 7814.3(6)$ Å^3, $Z = 4$, $Dc = 1.573$ g/cm^3; $\mu = 1.183$ cm^{-1}; min. and max. absorption correction factors: 0.6912 and 0.7457, 2θmax $= 56.362°$; 224868 reflections measured, 19415 unique; $Rint = 0.0312$; number of data/restraint/parameters 19415/200/1001; $R1 = 0.0303$ [18295 ref. with $I > 2\sigma(I)$], $wR(F2) = 0.0686$ (all data); largest difference peak 1.933 e·Å^{-3}. Asymmetric unit contains two independent molecules. Both

cations exhibit a disorder between coordinated hydride or chloride ligand. For each one, the H/Cl ratio had been refined with complementary occupancy factors. A SbF_6 counterion has also been found to be disordered, concerned atoms have been included in the model in two sets of positions and refined with restrains in geometry and atomic displacement parameters.

Structural data for 14: $C_{39}H_{44.85}Cl_{0.15}F_6N_3OsPSb \cdot C_{39}H_{44.70}Cl_{0.30}F_6N_3OsPSb$; $Mr = 2040.98$; yellow prism, $0.083 \times 0.140 \times 0.180$ mm^3; monoclinic $P2_1/c$; $a = 27.612(4)$ Å, $b = 11.6966(18)$ Å, $c = 24.349(4)$ Å; $\beta = 94.223(4)°$; $V = 7843(2)$ Å^3, $Z = 4$, $Dc = 1.729$ g/cm^3; $\mu = 4.042$ cm^{-1}; min. and max. absorption correction factors: 0.5153 and 0.6655, 2θmax $= 57.378°$; 324467 reflections measured, 19814 unique; $Rint = 0.0396$; number of data/restraint/parameters 19814/18/1079; $R1 = 0.0322$ [18902 ref. with $I > 2\sigma(I)$], $wR(F2) = 0.0744$ (all data); largest difference peak 1.933 e·Å^{-3}. Asymmetric unit contains two independent molecules. Both cations exhibit a disorder between coordinated hydride or chloride ligand. For each one, the H/Cl ratio had been refined with complementary occupancy factors. A SbF_6 counterion and a *p*-cymene fragment have also been found to be disordered, concerned atoms have been included in the model in two sets of positions and refined with restrains in geometry and atomic displacement parameters.

Structural data for 17: $C_{31}H_{35}F_6N_4RuSb \cdot C_4H_{10}O$; $Mr = 874.57$; yellow plate, $0.140 \times 0.200 \times 0.420$ mm^3; triclinic $P\bar{1}$; $a = 10.3597(5)$ Å, $b = 16.0888(18)$ Å, $c = 21.7237(11)$ Å; $\alpha = 85.2910(10)°$, $\beta = 80.1320(10)°$, $\gamma = 87.9280(10)°$; $V = 3554.3(3)$ Å^3, $Z = 4$, $Dc = 1.634$ g/cm^3; $\mu = 1.250$ cm^{-1}; min. and max. absorption correction factors: 0.6842 and 0.7902, 2θmax $= 60.558°$; 60272 reflections measured, 19504 unique; $Rint = 0.0214$; number of data/restraint/parameters 19504/2/800; $R1 = 0.0348$ [16831 ref. with $I > 2\sigma(I)$], $wR(F2) = 0.0839$ (all data); largest difference peak 1.623 e·Å^{-3}. One of the counterions has been found to be disordered. Involved atoms have been modelled with two sets of positions. Solvent

(diethylether) contribution to calculated structure factors has been calculated with SQUEEZE program.

Structural data for 19: $C_{35}H_{41}F_6N_4O_2RuSb \cdot C_4H_8O$; $Mr = 958.64$; yellow plate, $0.055 \times 0.075 \times 0.120$ mm^3; orthorhombic $P2_12_12_1$; $a = 11.6436(8)$ Å, $b = 15.5640(11)$ Å, $c = 21.8392(15)$ Å; $V = 3957.7(5)$ Å^3, $Z = 4$, $Dc = 1.609$ g/cm^3; $\mu = 1.134$ cm^{-1}; min. and max. absorption correction factors: 0.5833 and 0.7457, 2θmax $= 56.604°$; 52333 reflections measured, 9779 unique; $Rint = 0.0651$; number of data/restraint/parameters 9779/0/493; $R1 = 0.0411$ [7702 ref. with $I > 2\sigma(I)$], $wR(F2) = 0.0983$ (all data); largest difference peak 0.890 e·Å^{-3}.

———————

S2   SAINT+, *version 6.01: Area-Detector Integration Software*, Bruker AXS, Madison, WI, **2001**.

S3   (a) R. H. Blessing, *Acta Crystallogr.*, 1995, **A51**, 33-38. (b) SADABS, *Area Detector Absorption Correction Program*, Bruker AXS, Madison, WI, **1996**.

S4   (a) G. M. Sheldrick, *Acta Crystallogr.,* 1990, **A46**, 467-473. (b) G. M. Sheldrick, *Acta Crystallogr.,* A short history of SHELX. 2008, **A64**, 112-122.

S5   G. M. Sheldrick, *Acta Crystallogr.*, 2015, **C71**, 3-8.

S6   L. J. Farrugia, *Acta Crystallogr.*, 2012, **45**, 849-854.

S7   O. V. Dolomanov, L. J. Bourhis, R. J. Gildea, J. A. K. Howard and H. Puschmann, *J App. Cryst.,* 2009, **42**, 339-341.

S8   A. G. Orpen, *J. Chem. Soc., Dalton Trans.*, 1980, 2509-2516.

S9   R. H. Blessing, *Crystallogr. Rev.*, 1987, **2**, 3-58.

S10 A. L. Spek, *Acta Crystallogr. C,* 2015, **71**, 9-18.

8 Molecular structures of complexes 2, 4, 6 and 14

Crystal structure of complex 2

Fig. S5 Molecular structure of the cation of the complex **2**. For clarity all the hydrogen atoms are omitted, except those of NH groups.

Table S4 Selected bond lengths (Å) and angles (º) for complex **2**

Os-Ct[a]	1.7183(2)	S(1)-Os-P(1)	91.77(4)
Os-Cl	2.4101(13)	Cl-Os-S(1)	89.69(5)
Os-S(1)	2.4308(13)	Cl-Os-P(1)	86.18(4)
Os-P(1)	2.3345(12)	P(1)-Os-S(1)	91.77(4)
Ct-Os-Cl	123.23(1)	Os-S(1)-C(25)	117.74(18)
Ct-Os-S(1)	122.79(1)	N(1)-C(25)	1.329(6)
Ct-Os-P(1)	131.15(1)	N(2)-C(25)	1.333(6)

[a]Ct is the centroid of the ring of the Cym ligand

*Crystal structure of complex **4***
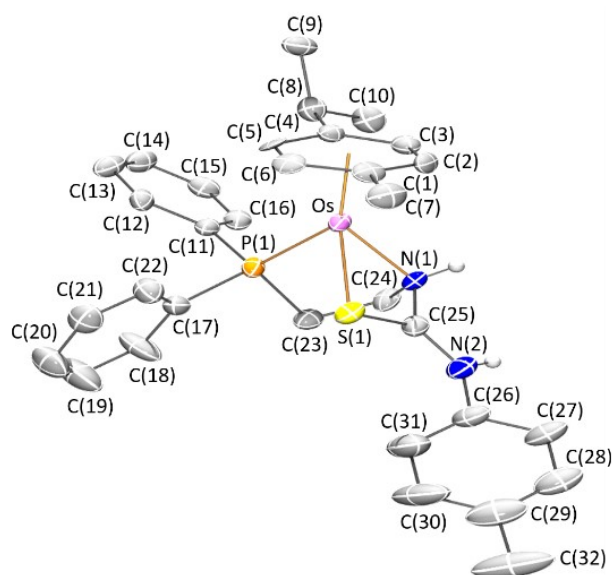
Fig. S6 Molecular structure of the cation of the complex **4**. For clarity all the hydrogen atoms are omitted, except those of NH groups.

Table S5 Selected bond lengths (Å) and angles (º) for complex **4**

Os-Ct^a	1.7188(1)	S(1)-Os-N(1)	68.21(14)
Os-S(1)	2.4014(18)	P(1)-Os-N(1)	81.59(14)
Os-P(1)	2.3072(16)	Os-S(1)-C(25)	83.4(2)
Os-N(1)	2.179(5)	S(1)-C(25)-N(1)	110.0(4)
Ct-Os-S(1)	130.62(1)	Os-N(1)-C(25)	97.7(4)
Ct-Os-P(1)	133.70(1)	N(1)-C(25)	1.449(8)
Ct-Os-N(1)	134.25(1)	N(2)-C(25)	1.293(8)
S(1)-Os-P(1)	85.31(6)		

^{a}Ct is the centroid of the ring of the Cym ligand
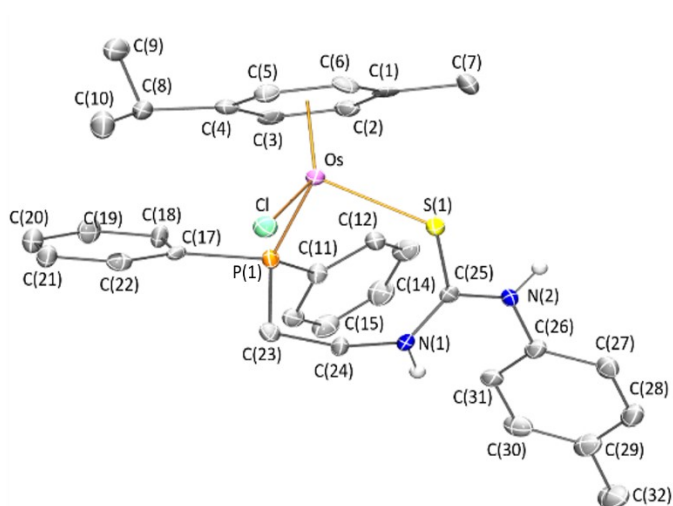
Crystal structure of complex 6
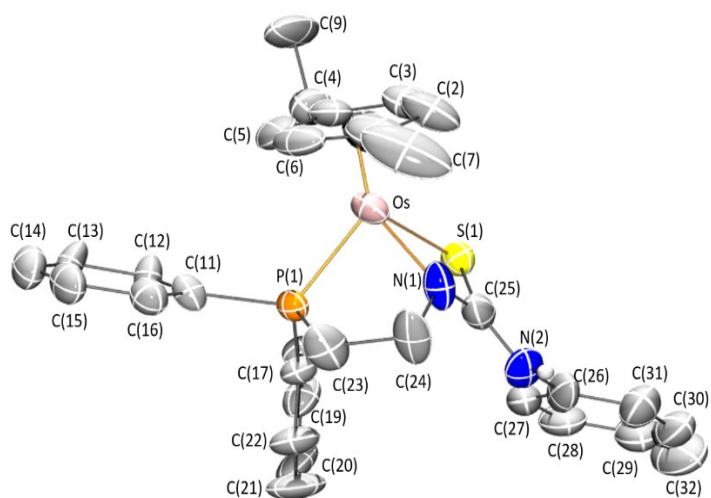
Fig. S7 Molecular structure of the cation of the complex **6**. For clarity all the hydrogen atoms are omitted, except that of NH bond.

Table S6. Selected bond lengths (Å) and angles (º) for complex **6**.

Os-Ct[a]	1.7068(1)	Os-S(1)-C(25)	81.9(5)
Os-S(1)	2.401(3)	S-C(25)-N(1)	106.5(9)
Os-P(1)	2.317(3)	S-C(25)-N(2)	126.3(11)
Os-N(1)	2.078(11)	N(1)-C(25)-N(2)	127.2(12)
Ct-Os-S(1)	129.43(1)	Os-N(1)-C(24)	124.1(8)
Ct-Os-P(1)	132.42(1)	Os-N(1)-C(25)	104.5(8)
Ct-Os-N(1)	135.10(1)	C(24)-N(1)-C(25)	118.4(12)
S(1)-Os-P(1)	94.50(10)	N(1)-C(25)	1.353(16)
S(1)-Os-N(1)	66.5(3)	N(2)-C(25)	1.349(16)
P(1)-Os-N(1)	73.5(3)		

[a]Ct is the centroid of the ring of the Cym ligand.

Table S7 Selected bond lengths (Å) and angles (º) for the second independent cation of complex **13** (structural parameters for the first independent cation are collected in Figure 3 caption)

M-Ct(1)[a]	1.7459(1)
M-P(1)	2.2617(6)
M-N(1)	2.1135(18)
M-H(1A)	1.527
Ct(1)-M-P(1)	134.69(1)
Ct(1)-M-N(1)	127.78(1)
Ct(1)-M-H(1)	129
P(1)-M-N(1)	81.57(5)
P(1)-M-H(1)	91.2
N(1)-M-H(1)	68.6
M-N(1)-C(25)	124.70(16)
N(1)-C(25)-N(2)	118.4(2)
N(1)-C(25)-N(3)	122.0(2)
N(2)-C(25)-N(3)	119.6(2)
N(1)-C(25)	1.309(3)
N(2)-C(25)	1.419(3)
N(3)-C(25)	1.369(3)

[a]Ct is the centroid of the ring of the Cym ligand.

Crystal structure of complex 14
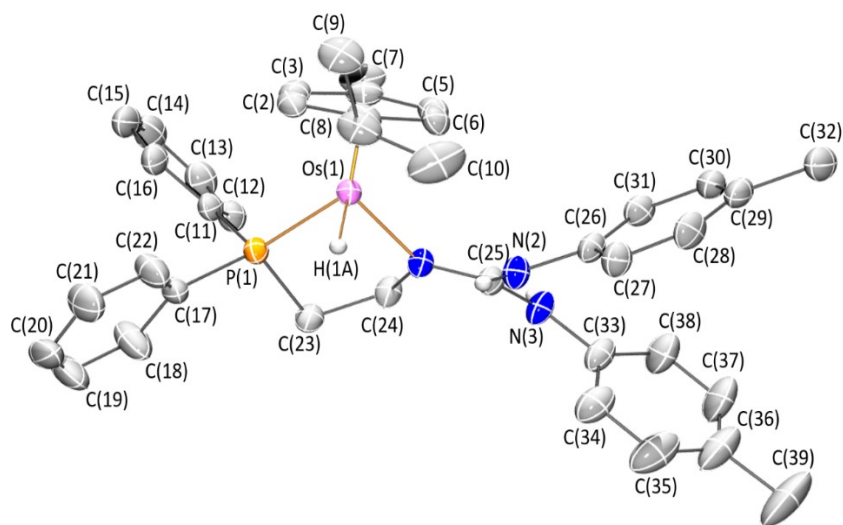
Fig. S8 Molecular structure of one of the chemically equivalent but crystallographically independent cations of the complex **14**. For clarity all the hydrogen atoms are omitted (except hydrido and those of NH bonds) together with minor components of disordered fragments have been omitted.

Table S8 Selected bond lengths (Å) and angles (º) for complex **14**

	Cation 1	**Cation 2**
M-Ct(1)[a]	1.7219(3)	1.7549(3)
M-P(1)	2.2909(9)	2.2783(10)
M-N(1)	2.127(3)	2.119(3)
M-H(1A)	1.605	1.606
Ct(1)-M-P(1)	133.58(1)	136.11(1)
Ct(1)-M-N(1)	129.82(1)	126.94(1)
Ct(1)-M-H(1)	121	124
P(1)-M-N(1)	80.80(8)	80.93(9)
P(1)-M-H(1)	87.9	84.6
N(1)-M-H(1)	89.2	89.0
M-N(1)-C(25)	125.4(2)	125.2(3)
N(1)-C(25)-N(2)	119.3(3)	118.8(4)
N(1)-C(25)-N(3)	122.0(3)	121.8(4)
N(2)-C(25)-N(3)	118.7(3)	119.4(4)
N(1)-C(25)	1.308(4)	1.308(5)
N(2)-C(25)	1.355(4)	1.356(5)
N(3)-C(25)	1.368(5)	1.366(5)

[a]Ct is the centroid of the ring of the Cym ligand.

Table S9 Selected bond lengths (Å) and angles (º) for the second independent cation of complex **17** (structural parameters for the first independent cation are collected in Figure 5 caption)

	Cation
Ru-Ct[a]	1.7136(1)
Ru-N(1)	2.0912(19)
Ru-N(2)	2.0833(19)
Ru-C(19)	2.065(2)
Ct-Ru-N(1)	128.14(1)
Ct-Ru-N(2)	132.74(1)
Ct-Ru-C(19)	128.10(1)
N(1)-Ru-N(2)	75.95(8)
N(1)-Ru-C(19)	90.17(8)
N(2)-Ru-C(19)	84.45(8)
N(2)-C(17)	1.305(3)
N(3)-C(17)	1.357(3)
N(4)-C(17)	1.371(3)

[a]Ct is the centroid of the ring of the Cym ligand

9 DFT calculations

Computational details

DFT geometry optimizations and thermochemical calculations were carried out with the Gaussian 09 program package,[S11] using the B3LYP-D3 dispersion-corrected hybrid functional.[S12] Geometry optimizations were performed in solution using the continuum SMD model,[S13] with dichloromethane ($\varepsilon = 8.93$) as solvent in the fluxionality studies of complexes **2** and **5**, or tetrahydrofuran ($\varepsilon = 7.4257$) in the reaction pathways of **7**. Basis sets used were the LanL2TZ(f) effective core potential basis set for the transition metal atoms, and the 6-311G(d,p) basis set for the remaining ones. The LanL2TZ(f) basis set is based in the Hay-Wadt relativistic effective core potentials (RECPs) for the transition metal atoms.[S14] All minima (no imaginary frequencies) and transition states (one imaginary frequency) were characterized by calculating the Hessian matrix. ZPE and gas-phase thermal corrections (entropy and enthalpy, 298.15 K, 1 atm) from these analyses were calculated. The transition state search was performed with a relaxed PES scan of the key geometrical parameter and then the highest energy structure was optimized as a transition state by the default Gaussian 09 algorithms. The chemical correctness of the transition states found were confirmed by visual inspection of the normal mode having a negative vibrational frequency, followed by moving the TS geometries along the reaction path using the GaussView program utilities and reoptimizing to verify the nature of the products.

S11 Gaussian 09 (Revision D.01): Frisch, M. J.; Trucks, G. W.; Schlegel, H. B.; Scuseria, G. E.: Robb, M. A.; Cheeseman, J. R.; Scalmani, G.; Barone, V.; Mennucci, B.; Petersson, G. A.; Nakatsuji, H.; Caricato, M.; Li, X.; Hratchian, H. P.; Izmaylov, A. F.; Bloino, J.; Zheng, G.; Sonnenberg, J. L.; Hada, M.; Ehara, M.; Toyota, K.; Fukuda, R.; Hasegawa, J.; Ishida, M.; Nakajima, T.; Honda, Y.; Kitao, O.; Nakai, H.; Vreven, T.; Montgomery, J. A. Jr.; Peralta, J. E.; Ogliaro, F.; Bearpark, M.; Heyd, J. J.; Brothers, E.; Kudin, K. N.; Staroverov, V. N.; Kobayashi, R.; Normand, J.; Raghavachari, K.; Rendell, A.; Burant, J. C.; Iyengar, S. S.; Tomasi, J.; Cossi, M.; Rega, N.; Millam, J. M.; Klene, M.; Knox, J. E.; Cross, J. B.; Bakken, V.; Adamo, C.; Jaramillo, J.; Gomperts, R.; Stratmann, R. E.; Yazyev, O.; Austin, A. J.; Cammi, R.; Pomelli, C.; Ochterski, J. W.; Martin, R. L.; Morokuma, K.; Zakrzewski, V. G.; Voth, G. A.: Salvador, P.; Dannenberg, J. J.;

Dapprich, S.; Daniels, A. *D.; Farkas, Ö.; Foresman, J. B.; Ortiz, J. V.; Cioslowski, J.;* Fox, D. J. Gaussian, Inc., Wallingford CT, 2009.

S12 (a) C. Lee, W. Yang and R. G. Parr, *Phys. Rev. B*, 1988, **37**, 785-789. (b) A. D. Becke, *J. Chem. Phys.*, 1993, **98**, 1372-1377. (c) A. D. Becke, *J. Chem. Phys*., 1993, **98**, 5648-5652. (d) S. Grimme, J. Antony, S. Ehrlich and H. Krieg, *J. Chem. Phys*., 2010, **132**, 154104.

S13 S. A. V. Marenich, C. J. Cramer and D. G. Truhlar, *J. Phys. Chem. B*, 2009, **113**, 6378.

S14 L. E. Roy, P. J. Hay, R: L. Martin, *J. Chem. Theory Comput.*, 2008, **132**, 1029-1031.